TECHNICAL REPORT OF THE JOINT RESEARCH WORK ON VOLCANIC ACTIVITIES IN THE PHILIPPINES

FEBRUARY 1981

JAPAN INTERNATIONAL COOPERATION AGENCY

C O N T E N T S

Preface

In response to a request of the Government of the Republic of the Philippines, the Government of Japan decided to conduct a survey on the current state of the activity of Taal Volcano, and entrusted the Japan International Cooperation Agency with the work. The JICA dispatched for the survey two experts, Dr. Yosihiro SAWADA (Volcano Physics) and Mr. Toshio MORI (Geophysics), to the Philippines from January 10 to February 20, 1980.

The experts conducted a joint survey and had discussions with their counterparts of the Philippine Commission on Volcanology, National Science Development Board of the Government of the Philippines. Based on the findings of the survey and further studies subsequently made in Japan, they have compiled this report.

I hope this report will contribute to the timely warning of volcanic eruptions and the protection of human lives from them as well as to the promotion of the friedly relations between our two countries.

I wish to express my deep appreciation to the officials concerned in the Philippines for their close cooperation extended to the experts.

March 1981

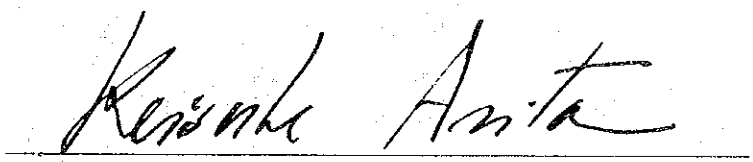

Keisuke ARITA
President
Japan International
Cooperation Agency

Abstract

The Joint Research Work on volcano-physical investigations between the Japanese government and the Philippine Commission on Volcanology, National Science Development Board, the Philippines was conducted during the period since January 10 through February 20, 1980.

The major purpose of this research work is to study the current state of volcanic activity at volcano Taal by operations of volcano-physical inspections. Seismological, geothermal and geomagnetic measurements were carried out and the brief of obtained results are as follows;

By seismological inspection by means of a portable seismograph, unequal distribution of amplitude of ground-tremor inside this volcano is confirmed. The amplitude of ground-tremor is larger in the western side of this volcano, the area including the last erupting site, and has been getting rather smaller since 1977.

By geothermal inspection by means of a portable infrared thermometer, it is confirmed that major high temperature areas are also distributed in the western side. Heat flux of volcano Taal is estimated to be 3.24×10^6 cal/ sec by the method proposed by Sekioka & Yuhara (1974), assuming the high temperature area as steaming ground.

By geomagnetic inspection by mean of a proton magnetometer, remarkable magnetic anomalies are found on and near the volcano island. The positive anomalous area in the south-western side overlaps the high temperature area.

Judging from these results, we conclude that volcano Taal is now in ordinary state, but still active from the viewpoint of geothermal activity.

Similar measurements by a seismograph and a magnetometer are also carried out at two volcanoes, Mayon and Bulusan, but remarkable volcanological events are not obtained by the field inspections. Volcano Mayon is in calm state in recent year. Volcano Bulusan, however is in its eruptive activity and a distinguished explosion-tremor recorded with the seismograph of the COMVOL is analyzed to estimate energy-release.

Yosihiro Sawada and Toshio Mori, Seismology and Volcanology Division, Meteorological Research Institute, 1-1 Nagamine, Yatabe, Tsukuba, Ibaraki 305, Japan

§1. Introduction

There are ten-odd active volcanoes in the Philippines as shown in Fig.1-1. Three-four volcanoes have shown eruptive activities or extra-ordinary state such as earthquake-swarms and increasings of plume-rising

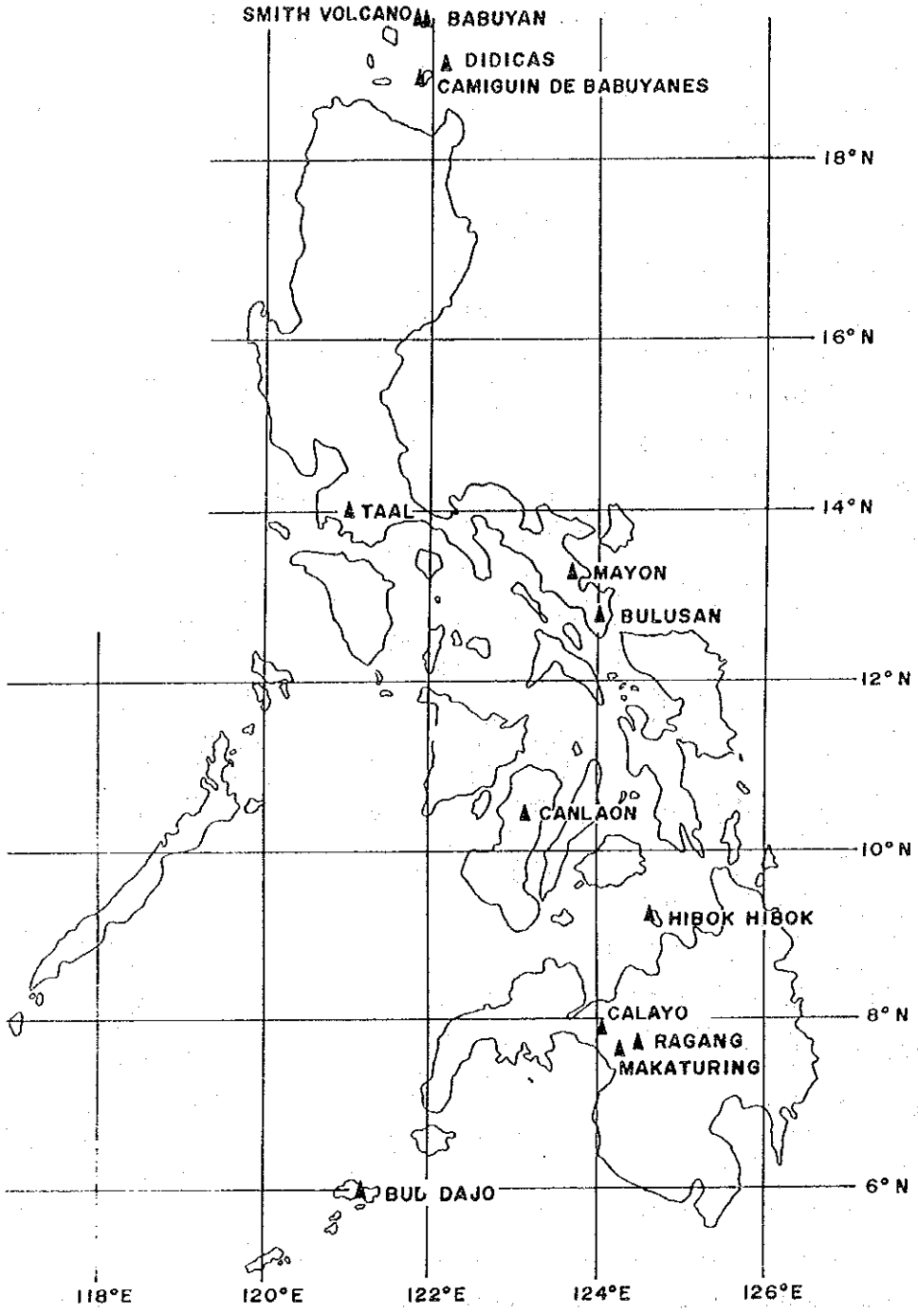

Fig. 1-1 Map showing the most active volcanoes in the Philippines. (after the Commission on Volcanology, Annual Report (1980))

every year. The Philippine Commission on Volcanology, the National Science Development Board (COMVOL) has operated the nation-wide volcanological surveillance at active volcanoes to prevent volcanic disasters in the Philippines.

The observatories are equipped with seismographs and water-tube tiltmeters and routine observations such as thermal measurements of high temperature areas, geochemical analysis of water samples, visual observations of active craters and periodical measurements by gravimeters & magnetometers have been operated.

Of the active volcanoes in the Philippines, volcano Taal (sometimes called as Volcano Island, 14°00'N, 121°00'E, 300 m a.s.l.) is one of the most dangerous volcanoes where is located in high populated region. This volcano violetly exploded in 1965 and caused severe damage by the strong phreato-magmatic explosions accompanied by base-surge[1),(2)], then the magmatic eruptions in 1968-1969 produced a large amount of lava flows. In recent years, volcano Taal showed frequent eruptions and the last activity took place in 1977, as shown in Table 1-1.

Table 1-1 Volcanic eruptions of volcano Taal since 1965.

Date	Duration	Strength	Feature
1965 Sept. 28-30	3 days	violent	Fissure. Phreato-magmatic. Base-surge.
1966 July 5-Aug. 5	31	moderate	Phreato-magmatic.
1967 July 16-19	3	mild	Phreatic.
1968 Jan. 31-Apr. 2	62	moderate	Magmatic. Lava flow.
1969 Oct. 29-Dec. 9	42	moderate	Magmatic. Lava flow.
1970 Nov. 19-23	5	mild	Phreato-magmatic.
1976 Sept. 3-Oct. 22	50	moderate	Phreatic. Fissure.
1977 Oct. 3-4	2	mild	Phreatic.

To judge the current volcanic activity of volcano Taal, the Joint Research Work between the Japan and the Philippines with geophysical techniques was conducted during the period since January 10 through February 20, 1980. Both of writers could attend this program and conduct respective inspections with staff-members of the COMVOL.

To operate volcano-physical inspections to investigate the volcanic activity of volcano Taal, seismological, geothermal and geomagnetic measurements were carried out with one seismograph, one infrared thermometer (IR thermometer) and one proton magnetometer.

To detect the active area with measurements of amplitude-distribution of ground tremor around active craters of volcano Taal was tried by field inspections with a portable seismograph. To detect high temperature areas and to estimate heat flux out of this volcano were tried by measurements of surface temperatures with a portable IR thermometer. And to estimate the underground geomagnetic structure was tried by measurements of the geomagnetic total intensity with a portable proton magnetometer.

Additional inspections by the same instruments were conducted at volcanoes Mayon (13°15'N, 123°41'E, 2990 m a.s.l.) and Bulusan (12°46'N, 124°30'E, 1559 m a.s.l.) to detect volcanic events, but unfortunately no remarkable phenomena were recorded during the temporary measurements at both volcanoes.

Brief of our conclusions and recommendation obtained by the Joint Research Work were already reported by our preliminary reports [8], [4], and we express herewith technical results of geophysical inspections conducted during this Joint Research Work.

Items of Seismological Inspection and Geothermal Inspection were written by Y. Sawada and item of Geomagnetic Inspection by T. Mori. The Joint Research Work was realized and supported by the Japanese Government and the Japan International Cooperation Agency under the Colombo Plan Technical Assistance Program.

§2. Seismological Inspection

1. Characteristics of Seismograph

(1) Seismograph equipped at volcanological observatory

Routine seismological observations by the COMVOL permanent observatories have been operated at designated active volcanoes in the Philippines. There are two observatories at volcano Taal, Pirapiraso (inside Taal volcano island) and Buco (shore of main land of Lake Taal), three observatories (Misericordia, Mayon Rest House and Tiwi) at Mayon volcano and one observatory (San Benon) at volcano Bulusan.

Electro-magnetic seismographs are settled at each observatory with following characteristics.

Type ; electro-magnetic & displacement (Hosaka Ltd., Japan)
Magnification ; 3000 - 5000
Period ; 1 sec.
Recording system ; smoked paper on drum recorder
Component ; three (two horizontal and one vertical)

(2) Portable seismograph

The writer brought one portable seismograph from Japan to conduct field measurements of volcanic events at three volcanoes during the Joint Research Work. The characteristics are as follows;

Type ; electro-magnetic & velocity
Amplifier ; three outputs (hand maded). the maximum gain ; 80 dB
Sensitivity ; 200 mv/m kine at 2 Hz
Transducer ; L-4C-V (Mark Products Ltd., U.S.A.). Vertical component 0.851 V/kine, Main coil;492 Ω, test coil;9.5 Ω, Period;0.96 Hz
Timing ; digital crystal clock
Recording ; 70-A Casset Data Recorder (TEAC Ltd., Japan), 4 channels
Power ; DC 12-24V (dry batteries)
Rerecording ; WTR-281 ink recorder (Watanabe Ltd., Japan)

A block diagram of the seismograph is illustrated in Fig. 2-1.

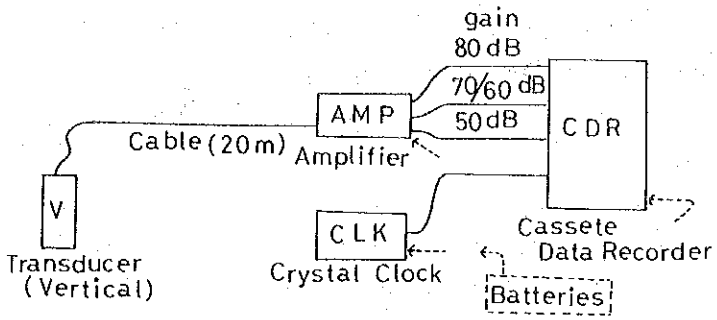

Fig. 2-1 Block-diagram of the portable seismograph used for this research work.

The overall response curve is shown in a left side of Fig. 2-2. The overall sensitivity and velocity & displacement magnification at a gain of 0.1 V/ cm rerecording at respective frequency are given in Table 2-1.

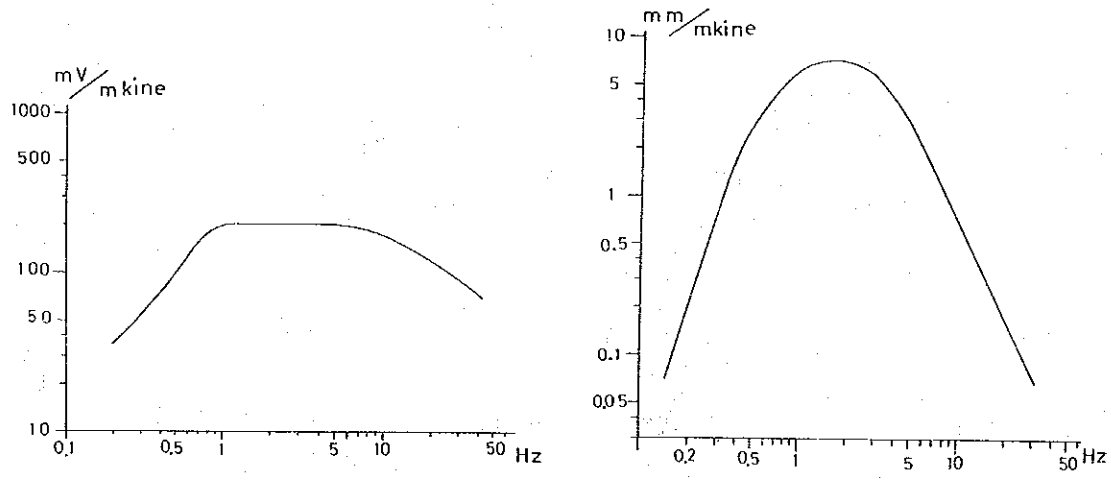

Fig. 2-2 Overall response curves for the portable seismograph (left) and the Ranger type seismograph (right).

Magnification was calculated based on the gain of the amplifier by using an oscillator, sensitivity of a transducer, rerecording gain of an ink-recorder and the equation (1). Velocity-sensitivity is calculated by an equation (2).

$$D = \frac{2\pi f \ Ia \ 10}{2\sqrt{2}\ e} \qquad (1)$$

where D; magnification (mm/mm)

f; frequency (Hz)

I; sensitivity of transducer (V/kine)

a; amplitude on recording paper at respective frequencies by an oscillator (mm) and

e; voltage of calibration signal (mV rms)

$$V = \frac{2\pi f \ 10^2}{D} \qquad (2)$$

where V; velocity sensitivity (m kine/mm)

f; frequency of signal (Hz) and

D; magnification (mm/mm)

Table 2-1 Overall sensitivity of the portable seismograph and its magnification in case of 0.1 V/cm rerecording.

Frequency	Sensitivity	Rerecording at 0.1 V/cm	
Hz	mV/m kine	μ kine / mm	mm/ mm
0.2	45.5	220	570
0.3	55.6	178	1060
0.4	71.4	140	1790
0.5	100.0	104	3030
0.6	125.0	76	4970
0.7	166.7	64	6960
0.8	166.7	60	8410
0.9	166.7	56	10040
1.0	200.0	54	11800
1.5	200.0	54	17700
2.0	200.0	54	23710
2.5	200.0	54	29720
3.0	200.0	54	35600
4.0	200.0	54	46900
5.0	200.0	54	57700
6.0	200.0	56	68800
7.0	166.7	56	78500
8.0	166.7	56	88700
9.0	166.7	58	98600
10.0	166.7	58	108400
15.0	142.9	66	143300
20.0	125.0	80	158200
30.0	90.9	110	172200

(3) Ranger type poratble seismograph

The COMVOL Main Office also operates temporary observations with portable seismographs in case of extra-ordinary & eruptive state of active volcanoes. At Bulusan, one temporary seismological station has been settled at Cogon owing to its eruptive activities since the end of

1979. At Taal, periodical measurements of volcanic tremor have been conducted since 1977 through 1979 to detect increasing activity after occurrence of the eruption in 1976.

The characteristics of the portable seismograph was obtained based on specific data and calibration-materials in the manual as follows;

Type ; PS-1A (Kinemetrix Ltd., U.S.A.)
Gain ; max: 2.0×10^6 mm/V
Transducer ; Ranger SS-1 (Kinemetrix Ltd., U.S.A.), Vertical/ Horizontal, 3.45 V/kine, Main coil; 5 kΩ Period 1.0 sec.
Writing system ; ink/ smoked-paper recording on drum recorder
Power ; DC (dry batteries)

Conditions of measurements at Taal and Bulusan were same as follows ;

Component ; vertical
Filter position ; No.1 (low pass, -3dB at 2Hz, 12dB/oct)
Pre-Amplifier ; -20 dB
Main Amplifier ; -36 dB
} - 56 dB in total
Low frequency cut-off position ; 0.5 Hz (-12 dB at 0.5 Hz, 24 dB/oct)
Sensitivity of a transducer ; 3.45 V/kine
The maximum gain of PS-1A ; 2.0×10^6 mm/V without attenuation

On the basis of the above-mentioned conditions and response curves in the manual of the seismograph, we can get the over-all response curve as shown in a right side in Fig. 2-2. In Table 2-2, velocity sensitivity and magnification at respective frequencies are given.

Table 2-2 Overall magnification of the Ranger type seismograph

Frequency	Velocity	Displacement
Hz	mkine/mm	mm/mm
0.15	12.94	7
0.2	5.14	25
0.3	1.29	145
0.4	0.58	440
0.5	0.36	860
0.6	0.27	1380
0.7	0.22	2020
0.8	0.19	2600
0.9	0.17	3280
1.0	0.16	3960
1.5	0.15	6500
2.0	0.15	8670
2.5	0.15	10230
3.0	0.18	10330
4.0	0.26	9750
5.0	0.36	8630
6.0	0.50	7500
7.0	0.65	6800
8.0	0.86	5820
9.0	1.09	5200
10.0	1.45	4340
15.0	3.25	2900
20.0	5.77	2180
30.0	13.67	1380

2. Seismological Observation at Pirapiraso Observatory, Volcano Taal

Pirapiraso observatory is located inside Taal volcano island, about 2.5 km N of a center of Main Crater (Fig. 2-3). An electromagnetic seismograph having three components is continuously operated by AC power supply by a gasolline generator.

Volcanic earthquakes and tremors are classified into six types as shown in Fig. 2-4 (Commission on Volcanology (1967)[5]). Of these classified volcanic events, a volcanic earthquake called "type S" has the clear secondary phase and represents the same wave forms of volcanic earthquake called as "A type" in Japan. "A type" volcanic earthquake is considered to occure at rather deep site under the active volcanoes.

In Table 2-3, monthly number of "S & SX" type earthquakes after 1976 detected at Pirapiraso observatory is shown. In Fig. 2-5, the monthly number

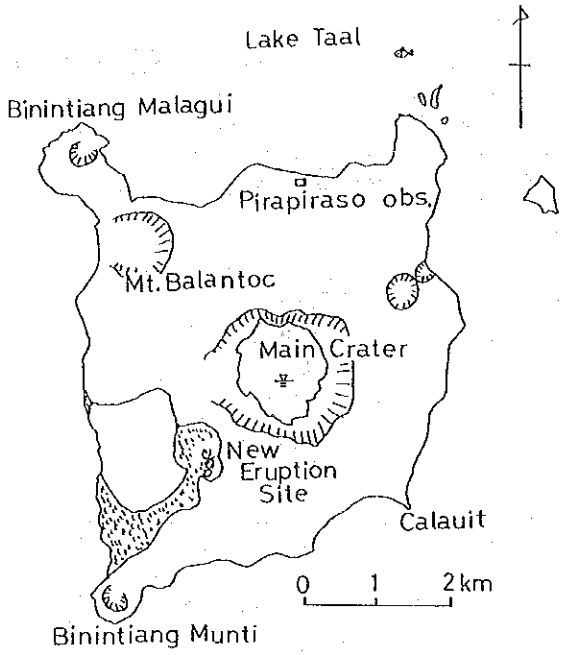

Fig. 2-3 Location of Pirapiraso Volcano Observatory, volcano Taal.

Table 2-3 Monthly frequency of volcanic earthquakes (type "S and SX") detected at Pirapiraso Volcano Observatory at volcano Taal during the period 1976~mid-1980 (by the seismological observation of the COMVOL).

Month	1976	1977	1978	1979	1980
Jan.	4	2	40	19	14
Feb.	14	2	59	17	1
Mar.	5	0	108	19	4
Apr.	0	2	92	7	8
May	0	4	118	27	29
June	2	0	57	11	12
July	0	3	11	12	12
Aug.	1	1	18	8	
Sept.	0	5	39	4	
Oct.	0	5	20	11	
Nov.	1	2	58	7	
Dec.	1	8	15	8	
Total	28	34	635	150	(80)
Monthly Average	2.33	2.83	52.92	12.50	(11.43)
Daily Average	0.08	0.09	1.74	0.41	(0.38)

Type "S" — 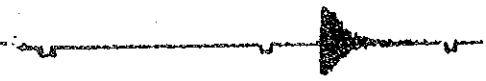

Characteristics: Sharp secondary, primary very close to secondary and usually not detectable, period of 0.2-0.3 *second, short duration.*

Type "b" — 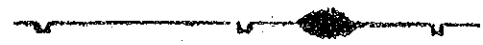

Characteristics: Short duration, almond-shaped, no distinct 'p' and 's', period same as "s" type.

Type "a" — 

Characteristics: Almond-shaped as in type "b" but the period is about 0.5 *second, short duration.*

Type "x" — 

Characteristics: A train or series of type "a" tremors the duration of which could be several minutes up to more than an hour. Can be distinguished from regular microseisms in the same record by its relatively larger double amplitudes and slightly bigger period.

Type "sx" — 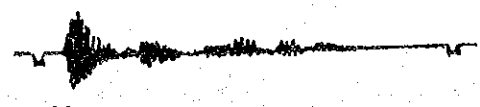

Characteristics: Sharp onset, larger vibrations are found at the start and then followed by several nodes of the same period but of decreasing maximum double amplitude. The average period of its vibrations is 0.5 *second.*

Type "E" — 

Characteristics: Asymmetrical spindle-shaped tremor of varying periods. The start is short-period with no distinct 'p' and the amplitude increasing toward the node. The node is composed of several vibrations whose period is bigger than front and tail of the spindle. The duration ranges from half a minute to two minutes. This type was designated "E" because it was the prominent type of tremor recorded in the 1966 *eruption of Taal.*

Fig. 2-4 Classification of volcanic earthquakes/volcanic tremors at volcano Taal.[5]

and moving average values every three months after 1976 are shown with histogram and dotted line, respectively.

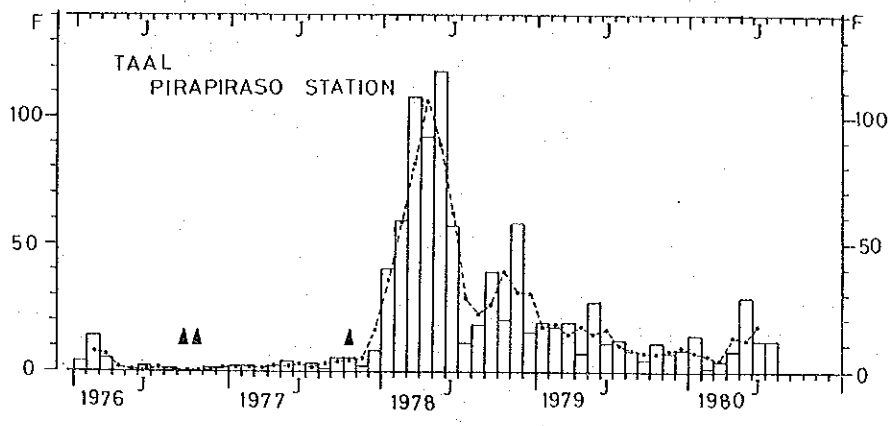

Fig. 2-5 Time variation of monthly frequency of volcanic earthquakes observed at Pirapiraso Observatory, during the period 1976 ~mid-1980. Triangular denotes occurence of volcanic eruption and dotted line denotes values of moving-average every three months.

It is clear that monthly frequency rapidly increased in 1978 but no eruption took place, and there were not remarkable bursts of volcanic earthquakes before & during eruptive activities in 1976 and 1977.

Frequency of occurrence of volcanic earthquakes since 1978 has decreased through 1980. However, comparing seismic activity at active volcanoes in Japan, the frequency of 11-12 per month or 0.4 per day of "type S" ("A type" in Japan) earthquakes belongs to rather high level.

3. Field Inspections by the Portable Seismograph at Volcano Taal

To detect ground vibration generated by volcanic activity and to investigate amplitude-distribution around active craters inside Taal volcano island, field inspections were conducted at 31 points in total, 1-31 as shown in Fig. 2-6. Measurement-sites were selected at locations from the shore to the center of the volcano island, Main Crater to elucidate amplitude-distribution inside this volcano island.

Field inspections were carried out on days when it was calm weather condition, especially no windy and no waves on the surface of Lake Taal, and

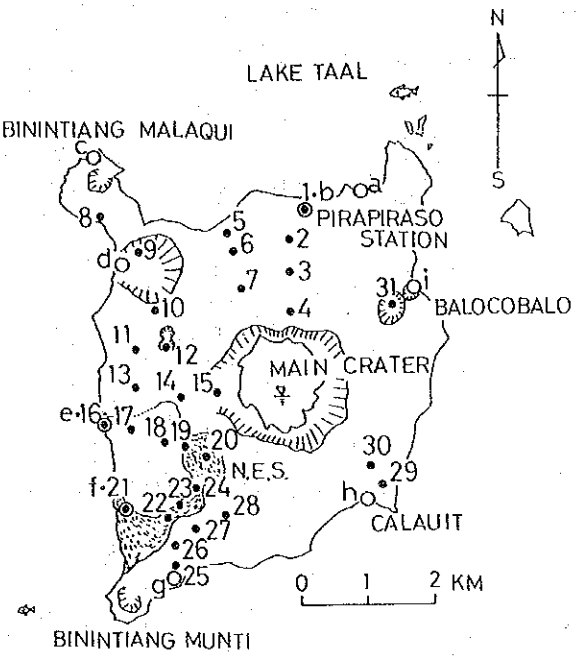

Fig. 2-6 Distribution of measurement sites (No. 1~31) for seismological inspections during this research work at volcano Taal.

at sites not near living areas & crop-fields to prevent disturbance of the noises.

Examples of rerecorded ground vibration at 31 points are given in Fig. 2-7. These records are processed by a spectrum band-pass (0.89-14.0 Hz, 32 dB/oct) with a function filter (JEIC (Densi-Sokki) Ltd., Japan) as shown in Fig. 2-8 to erase noise-vibrations of very short frequency and of rather long period.

It is clear that amplitude of ground vibrations at the western side of this volcano are larger than those observed in the eastern side. Waves of rather long period are still included in records at points of 1, 5, 13 and 16.

To investigate the frequency-characteristics of these obtained ground vibrations, analysis by the Fast Fourier Transform (FFT) of recorded waves were tried with the spectrum analyzer (model 3582A, Hewlett-Packard Ltd., U.S.A.). By this instrument, peak frequency within 25 Hz of each recorded ground-vibration was obtained by the FFT method from analog signals recorded in magnetic tapes. It, however, is hard to separate around DC signals from

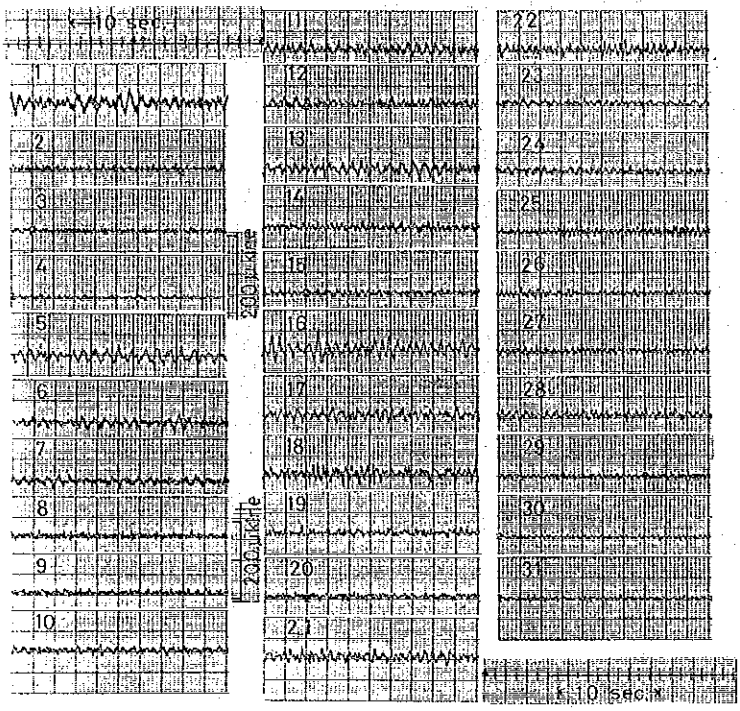

Fig. 2-7 Examples of rerecorded ground vibrations observed at 31 points at volcano Taal.

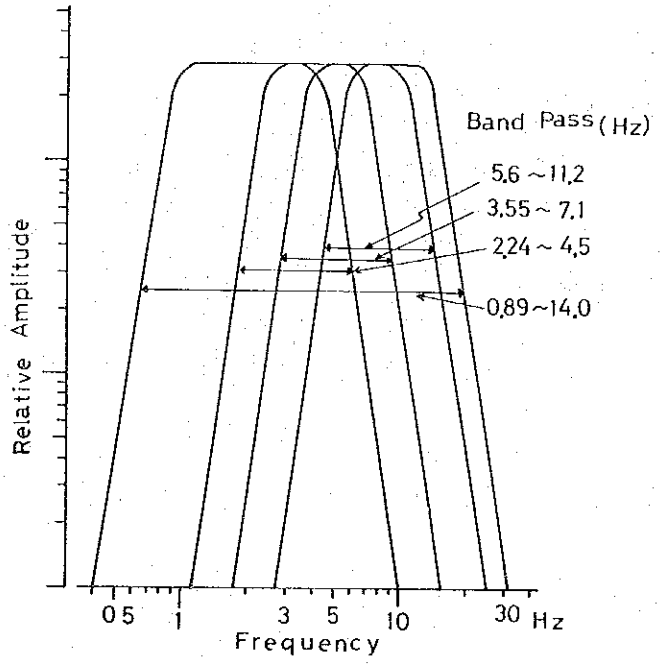

Fig. 2-8 Spectrum band-pass used for analysis of ground vibrations obtained at volcano Taal.

analyzed spectrum owing to the critical ability of this spectrum analyzer. When we investigate volcanic tremors with seismometers of 1 sec. period, signals of high frequency more than around 20 Hz are considered to be noises by artificial origins, and signals of low frequency under around one second are considered to be ground noises, especially disturbances generated by waves in case of an island volcano surrounded by a lake, such as Taal volcano. So, it will be tolerable to cut lower spectrum than one second for the purpose of analysis of volcanic tremor at volcano Taal. In Fig.2-9, examples of traces of spectrum analysis by the FFT with the spectrum analyzer between 1 and 25 Hz are shown. From these examples, we can see that peaks of sectrum of obtained ground vibrations (during 1 and 25 Hz) appear within around 8 Hz. High frequencies more than 10 Hz may be caused by artificial origins. Obtained mean amplitude (p-p & average during 3 minutes) and peak frequency (average of six analyzed results) at 31 points are shown in Table 2-4.

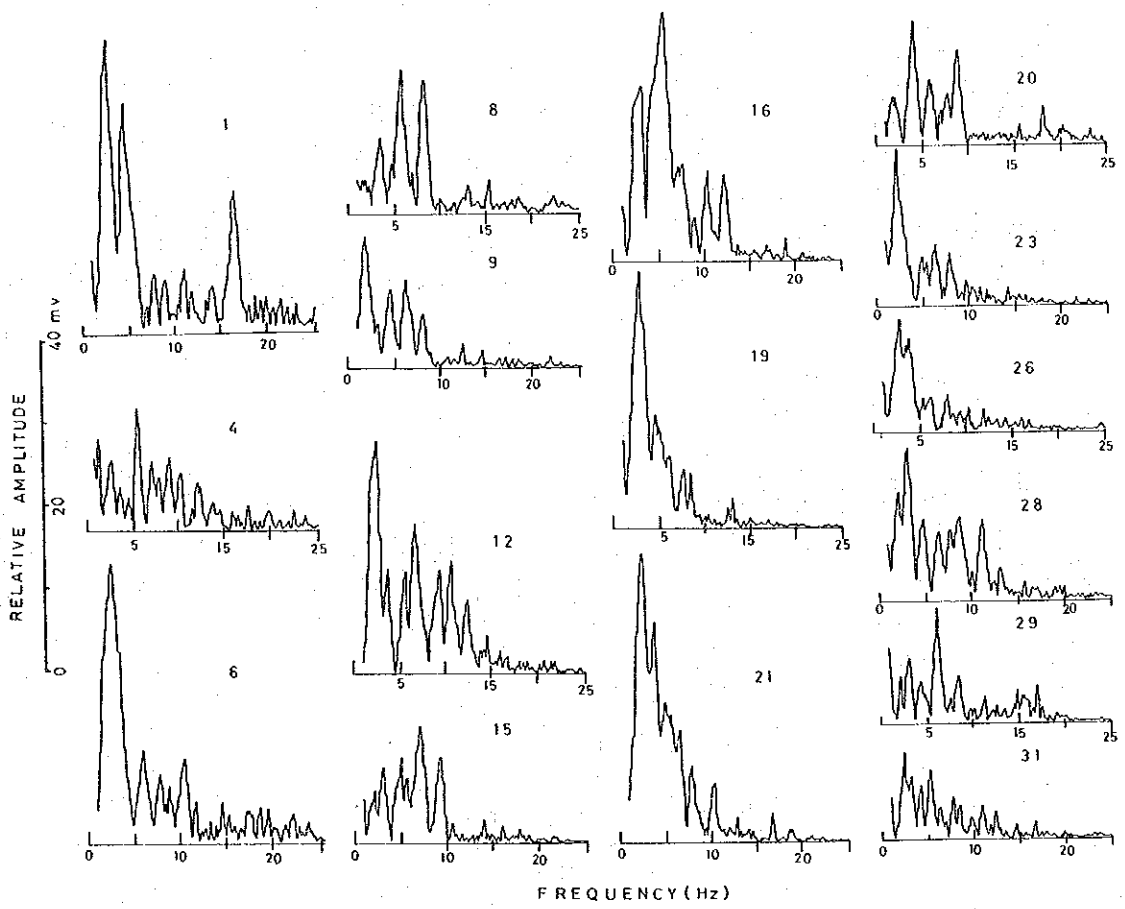

Fig. 2-9 Examples of the FFT spectrum of ground vibrations at volcano Taal. Numerical number denotes a measurement site.

Table 2-4 Mean amplitude and peak frequency of ground vibration obtained at volcano Taal by this seismological inspections.

Observation Spot	Date	Amplitude	Frequency
		μ kine	Hz
1	Jan.19	342	2.88
2	Jan.26	134	2.43
3	"	97	2.43
4	"	77	5.58
5	"	391	2.52
6	"	218	2.43
7	"	128	2.16
8	Jan.20	125	6.39
9	"	120	2.52
10	"	141	2.16
11	Jan.22	217	2.07
12	"	180	2.88
13	Jan.27	289	2.61
14	"	171	2.52
15	"	123	7.29
16	Jan.21	537	5.67
17	"	237	1.98
18	"	329	6.84
19	"	147	2.70
20	Jan.19	160	4.05
21	"	249	2.79
22	"	259	5.58
23	"	130	2.34
24	Jan.21	129	2.16
25	Jan.28	126	3.78
26	"	103	3.06
27	"	168	4.86
28	Jan.22	165	3.24
29	Jan.28	122	6.12
30	"	77	3.06
31	"	92	2.52

Peak frequencies in Table 2-4 are divided into three groups at around 3,5 and 8 Hz. To see amplitude variations at 31 observation sites near the above-mentioned three peak frequencies, analysis of three spectrum band-pass (from 2.24 to 4.5 Hz, from 3.55 to 7.1 Hz and from 5.6 to 11.2 Hz) as shown in Fig. 2-8 were tried, and the records filtered by each spectrum band-pass are shown in Fig. 2-10 and relative amplitude (p-p & mean amplitude during 1 minute) at each frequency range are also shown in Fig. 2-11. At the bottom in Fig. 2-11, amplitudes given in Fig. 2-7 are also shown.

By these analysis, we can see that large amplitude at respective frequency-range appearred at points of 16, 18, 19, 21 and 22 at 2.24-4.5 Hz,

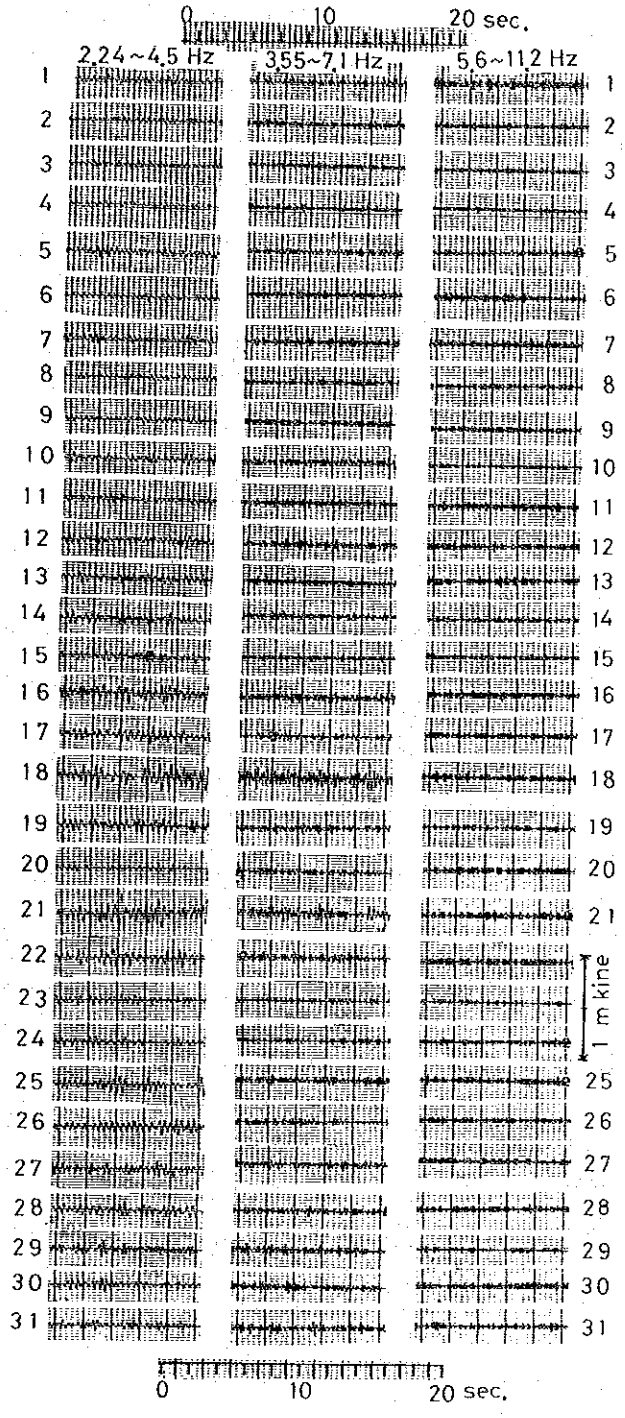

Fig. 2-10 Wave-forms of ground vibration at each spectrum band pass (shown at top of records).

1, 12, 16, 18, 19, 21 and 22 at 3.55-7.1 Hz and 1, 13, 16, 20, 21 and 22 at 5.6-11.2 Hz. In case of original records, large amplitude appearred at points of 1, 5, 13, 16, 18, 21 and 22 where almost of them is located near

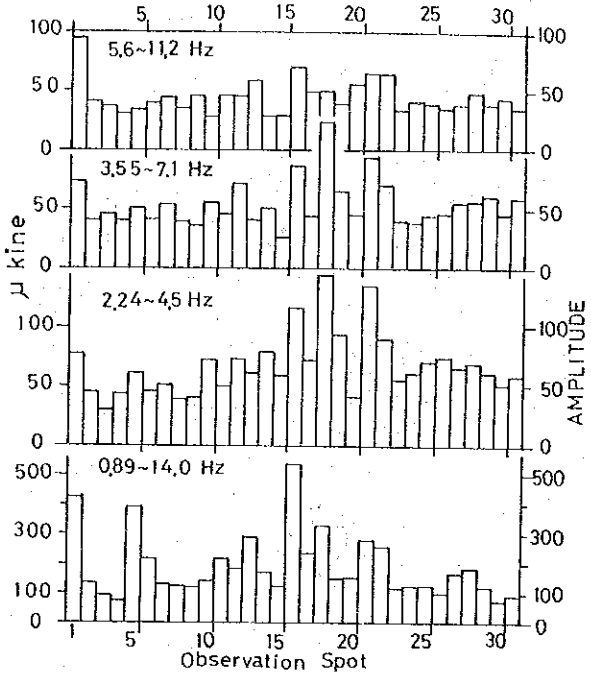

Fig. 2-11 Relative amplitude of ground vibration at 31 points at each spectrum band pass (shown in respective column)

the shore. So we have to consider that the large amplitude of ground vibration as shown in Fig. 2-7 will include disturbances of waves in Lake Taal.

However, according to results of filtered analysis by three spectrum band-pass filters, large amplitudes appearred at points of 16, 18, 19, 21 and 22 where are located around the New Eruption Site at the range of 2.24-4.5 Hz band-pass, as shown in Fig. 2-11. In case of band-pass analysis at 3.55-7.1 Hz and 5.6-11.2 Hz, same tendency is also seen at positions near the New Eruption Site, excepting positions at 1, 12 and 13 (Fig. 2-11).

Amplitude-distribution (in Table 2-4) inside volcano island is shown in Fig. 2-12. Though large amplitude area is located at the northern side, it is clear that the western side shows larger amplitude comparing the eastern side. Especially, large amplitude distribution appears near the area of the New Eruption Site. The New Eruption Site is the area where showed the latest eruptive activities, and these large amplitude-distributions may represent volcanic phenomena. But the following three features prevent to consider those ground vibrations as volcanic tremor; first, the largest amplitude does not appear around the locations near the craters which showed the latest eruptions and the activest geothermal anomalies at the New Eruption

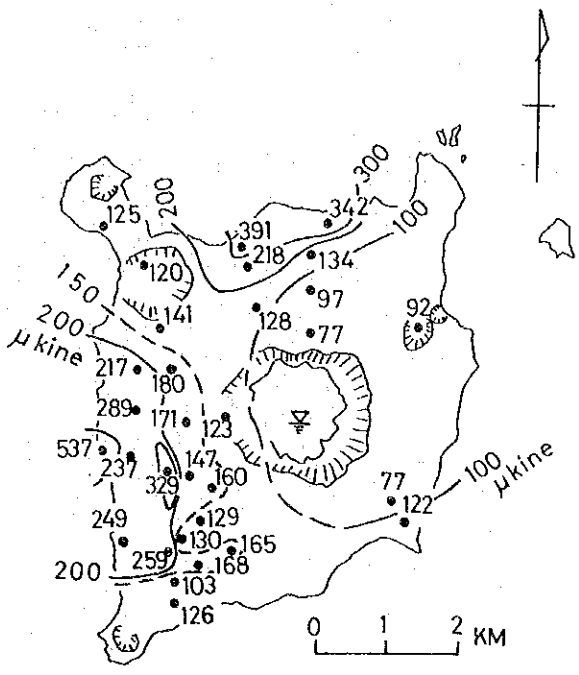

Fig. 2-12 Amplitude distribution of ground vibration obtained during this research work inside Taal volcano island (January, 1980).

Site. Second, it is difficult to consider that the amplitude distribution is generated by a single underground origin, because we can not find out the simple relationship between amplitude and distance from supposed site near/around Kaygabok. And then, peak frequencies of these ground vibrations are not uniform at every position.

So, the author cannot conclude that the ground vibrations obtained by field inspections during the research work are volcanic tremor, but could elucidate the unequal amplitude-distribution inside the volcano island as shown in Fig. 2-12.

This unequal distribution of amplitude of ground vibration may reflect the volcanic activities, but further detailed field inspections are necessary to make the problem clear.

4. Analysis of Seismogram Obtained with the Ranger type Seismograph

Field measurements by the Ranger type portable seismograph have been carried out by the COMVOL since 1977 through 1979 along the shore of this volcano. To study the past activity of volcanic tremor, the author read

amplitude & period of continuous waves recorded by the seismograph.

Over-all sensitivity during all observations was the same and is shown at the right side in Fig. 2-2 and Table 2-2, and the observation points are given as a~i in Fig. 2-6. Three points (b, e and f) of 9 points are the same as 1, 16 and 21 sites in this research work,

The field inspection around the volcano island on the same day was conducted on September 20, 1978 and tha maximum amplitude & the period and the mean amplitude (p-p) & the mean period during one minute of continuous waves read by the author are given in Table 2-5. The maximum amplitude (p-p) of waves was more than 1 m kine at that time at the point f (Kaygabok).

Table 2-5 The maximum and mean amplitude of continuous waves with the periods at volcano Taal detected with the Ranger type seismograph on September 20, 1978.

Observation Spot	Maximum	Period	Average	Period
	μ kine	sec.	μ kine	sec.
a Tabla	-	-	-	-
b Pirapiraso	73	0.7	46	0.62
c B. Malaqui	44	0.7	25	0.69
d Mt. Balantoc	394	0.7	242	0.70
e Alas-As	453	0.7	321	0.70
f Kaygabok	1160	0.65	531	0.57
g Saluyan	435	0.6	270	0.47
h Calauit	145	0.6	107	0.56
i Pinagulbuan	92	0.9	50	0.69

On the contrary, no trace was detected at the point a.

Frequency of respective period of waves at an interval of 0.1 sec. during one minute at b~i observation points is given in % in Fig. 2-13. Peak of period of each record varies between 0.4 and 0.9 sec., and mostly around 0.6 - 0.7 sec.. We can consider that values of these periods are different from ground vibration generated by waves of Lake Taal and by artificial origins.

Fig. 2-14 shows a distribution of mean amplitude given in Table 2-5. Unequal distribution of amplitude is clear inside this volcano island and amplitude of vibration is larger at the western side, especially around

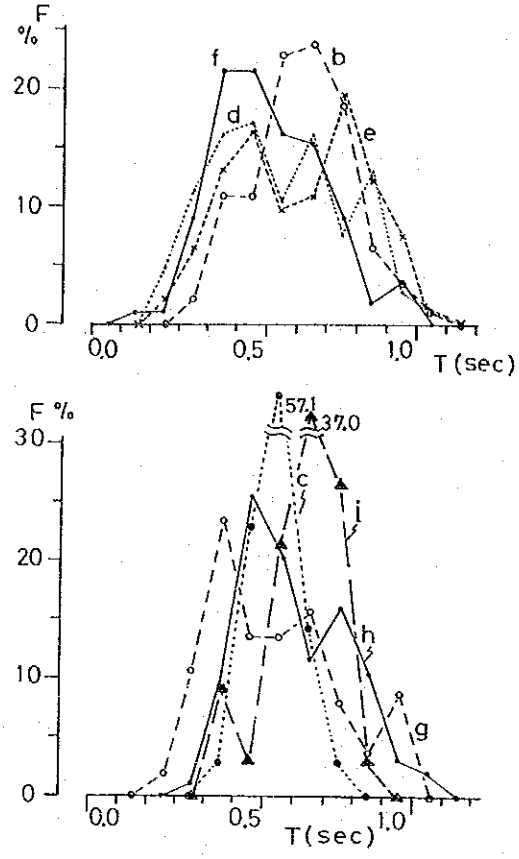

Fig. 2-13 Frequency of period of continuous waves observed at b~i points by the COMVOL on September 20, 1978.

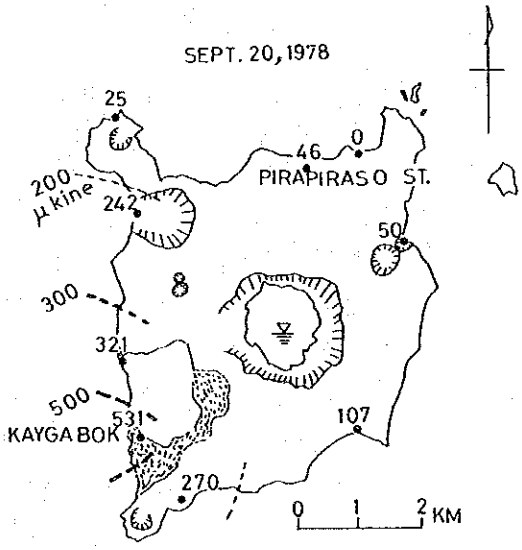

Fig. 2-14 Amplitude distribution of continuous waves observed inside Taal volcano island, observed on September 20, 1978.

Kaygabok where is the nearest site from the eruption crater in 1977. The general tendency of unequal distribution of amplitude inside the volcano island is similar as results obtained by the research work, excepting the northern part.

On the basis of the above-mentioned features of period & amplitude-distribution inside the volcano island, we are able to judge that the continuous waves are generated by volcanic activity. The COMVOL has continued the periodical measurements of the continuous waves (volcanic tremors) at Kaygabok, point f to monitor volcanic activity by time variations of wave-amplitude.

The writer read the continuous waves in seismograms of the periodical measurements conducted by Pirapiraso Observatory and mean amplitude (p-p) & mean period mean period during one minute are given in Table 2-6. The first six values (March 22 - August 3, 1977) were recorded by ink-recording, and the other by smoked paper writing.

Table 2-6 Mean values of amplitude and period of continuous waves obtained at Kaygabok, the SE side of volcano Taal during the period 1977 - 1979.

Date		Average	Period
		μ kine	sec.
1977	Mar. 22	153	0.61
	29	115	0.62
	Apr. 5	92	0.67
	May 18	126	0.60
	July 26	386	0.58
	Aug. 3	549	0.63
	27	511	0.45
	Sept 11	360	0.47
	Oct. 6	594	0.47
	Nov. 9	337	0.53
	Dec. 19	230	0.55
1978	Jan. 8	295	0.56
	Feb. 15	380	0.58
	Mar. 25	563	0.53
	Apr. 27	494	0.58
	May 18	450	0.51
	June 17	359	0.52
	July 16	280	0.53
	Aug. 23	335	0.59
	Sept.19	222	0.61
	20	531	0.57
	21	665	0.73
	Oct. 21	327	0.65
	Nov. 21	352	0.58
	Dec. 21	402	0.64
1979	Jan. 25	192	0.63
	Feb. 13	100	0.57
	Mar. 9	134	0.65

Time variations of the mean amplitude is shown in Fig. 2-15, and the mean value during the Joint Research Work (January 19, 1980) is also plotted with an open circle in this figure. Increase of large amplitude of continuous waves were observed before and during the small eruptions took place in October, 1977. And then, in general tendency, amplitudes of waves obtained at Kaygabok represent gradual decreasing through 1979, except a sharp increase in September, 1978. The value in 1980 belongs to a low amplitude of waves, too.

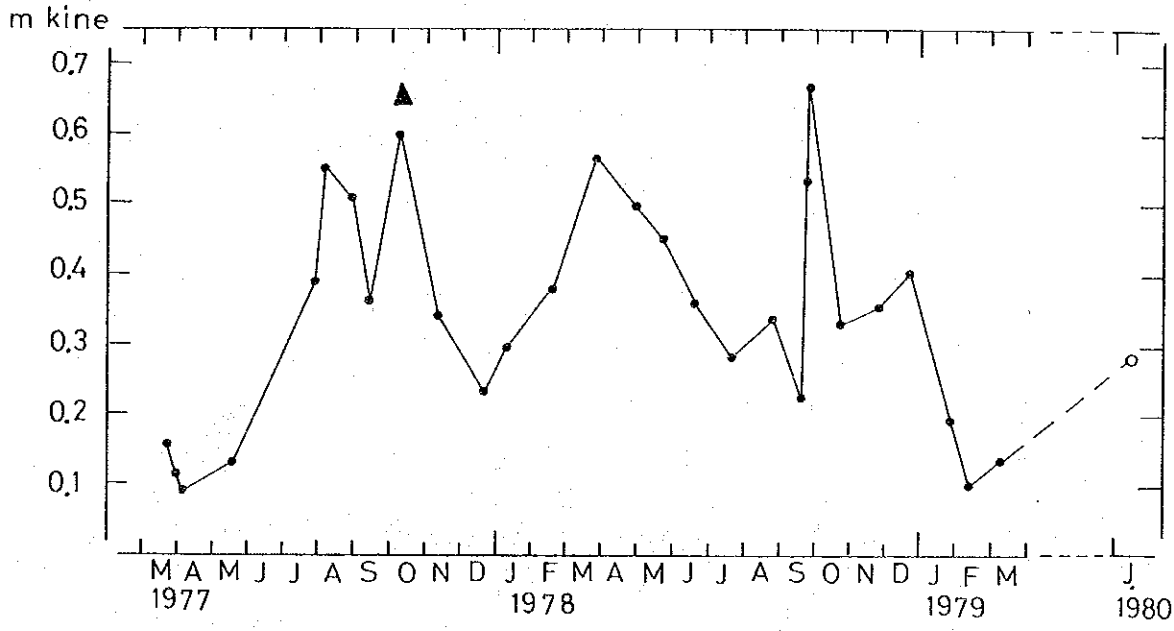

Fig. 2-15 Time variations of mean amplitude of continuous waves obtained at Kaygabok, volcano Taal during the period 1977-1979 by the COMVOL. Open circle in 1980 denotes a value at the same position by the portable seismograph on January 19, 1980 by this research work and triangular the volcanic eruption in October, 1977.

The general tendency of amplitude-decreasing of ground vibration at volcano Taal may represent the decreasing of volcanic activities of this volcano. Periodical inspections of ground vibration by a portable seismograph is considered to be one of very effective method to monitor volcanic activity of volcano Taal.

5. Ground Vibration at Volcano Mayon

Volcano Mayon was in calm state when we visited in early February, 1980. There are three volcano observatories of the COMVOL, Sta. Misericordia (ca. 10 km E of the summit crater), Mayon Rest House Station (ca. 4.1 km NNW of the crater) and Tiwi (ca. 17 km NNE of the crater) equipped with electromagnetic seismographs and water-tube tilt meters. Two of them are shown in Fig. 2-16.

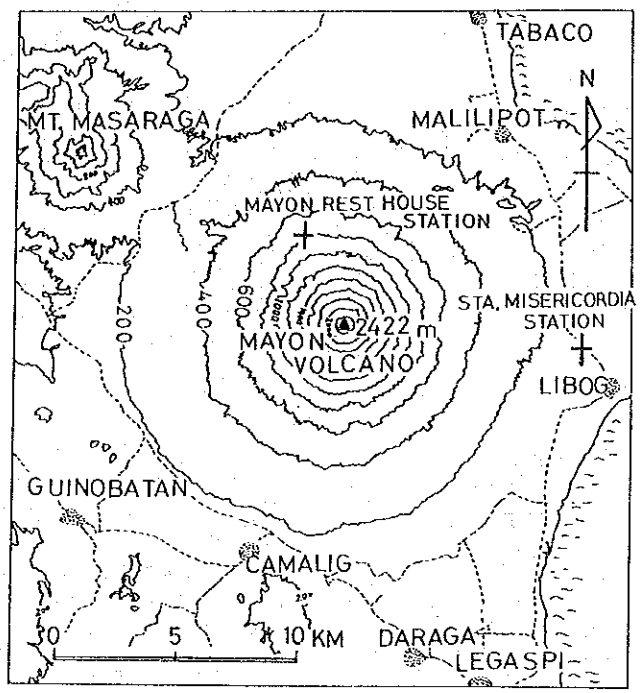

Fig. 2-16 Distribution of volcano observatories at volcano Mayon.

The writer conducted seismological inspections on February 5 and February 13, 1980 with the portable seismograph inside the transducer-shelter of the Mayon Rest House station. In active stage, characteristic volcanic tremors have been observed at volcano Mayon, but recent seismic activities of this volcano are in low frequency and the writer could not detect any volcanic events by these measurements.

Mean amplitude (p-p) of ground vibration was larger than ca. 200 μ kine and the wave frequency was around 5 Hz in the shelter as shown in Table 2-7. This observatory is situated at the altitude of about 800 m a.s.l. and it is usually windy. The above-mentioned amplitude belongs to rather large amplitude of ordinary ground tremor, but is mostly caused by rapid change of

Table 2-7 Ground vibration observed at volcano Mayon.

Date	Location	Mean amplitude	Frequency
Feb. 5	Mayon Rest House Station	218 μ kine	5.0-5.3 Hz
Feb.13	"	326	5.0-5.2
"	"	196	5.0-5.4

weather accompanied by winds during the inspections.

6. Ground Vibration at Volcano Bulusan

Volcano Bulusan has been in eruptive activity since the end of 1979 and still continued the eruptions at the summit craters during our inspections. There has been one volcano observatory at San Benon (ca. 5.3 km SSW of the summit craters) which is now rebuilt. Besides this observatory, another seismological observation point with the Ranger type seismograph has been temporally settled by the COMVOL Main Office since January 13, 1980 at Cogon (ca. 4.6 km WSW of the summit) to monitor seismic activities of this volcano. Locations of two stations are shown in Fig. 2-17.

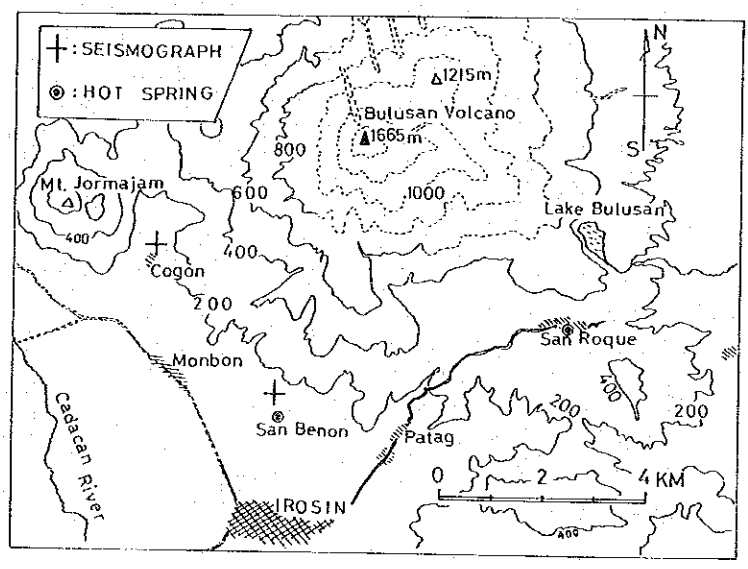

Fig. 2-17 Distribution map for seismograph stations and hot springs at the foot of volcano Bulusan.

Seismological inspections with the portable seismograph were conducted at the both sites in mid-February. Mean amplitude (p-p) during one minute and

the frequency of them are given in Table 2-8. At San Benon, rather large amplitude of ground vibration and rather high wave-frequency were observed,

Table 2-8 Ground vibration observed at volcano Bulusan.

Date	Location	Mean amplitude	Frequency
Feb. 9	San Benon	342 μ kine	6.7-10.0 Hz
Feb. 10	Cogon (near recorder)	220	5.0-6.7
"	"	275	5.0-6.7
"	Cogon (near transducer)	187	5.0-7.1
"	"	209	5.0-6.7
Feb. 11	"	283	5.0-5.6
"	"	103	3.3-7.1
Feb. 12	"	231	5.0-8.3
"	"	250	5.0

and they are mainly caused by artificial origins around the observatory. At Cogon, rather large amplitude of ground vibration was sometimes obtained, too. The seismograph is settled near the village, and rather large amplitude is because of the surrounding living activities.

7. Variations of Seismic Activity before Eruptive Activities of Volcano Bulusan

During the Joint Research Work, volcano Bulusan erupted on January 12 and on February 7, 8 and 9, 1980. Daily frequency of seismic events (volcanic earthquakes and volcanic tremors) obtained with the Ranger type seismograph settled at Cogon station during the period since January 13 through February 14 is given in Fig. 2-18.

According to the COMVOL observation, precursory swarm of volcanic earthquakes and volcanic tremors were recorded by seismographs at both stations, but unfortunately the author could not obtain those seismic events prior to & during eruptive activities by the seismological inspections, with the portable seismograph. Hatched histogram in Fig. 2-18 means "Type S" volcanic earthquakes and they frequently occurred prior to volcanic eruptions.

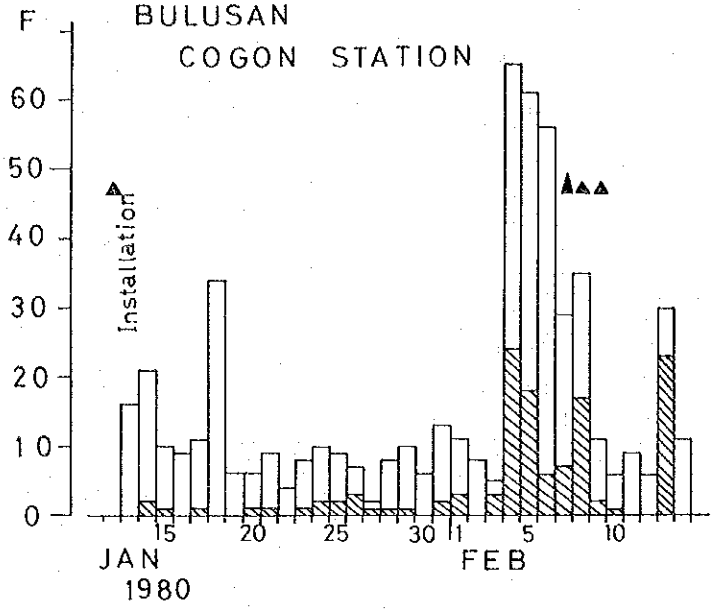

Fig. 2-18 Daily frequency of seismological events (earthquakes/tremors) detected at Cogon Station by the seismological observation by the COMVOL, at volcano Bulusan. Triangular denotes occurence of volcanic eruption and hatched histogram "type S" volcanic earthquake.

The COMVOL could use the occurrence of swarm of "type S" earthquakes as fairly clear precursory events of approaching eruption.

8. Analysis of the Explosion Tremor at 02:15 on February 7, 1980 of Volcano Bulusan

The explosion at 02:15 on February 7, 1980 was the strong one accompanied by ca. 6000 m high ash-plume, ash-fall in areas of the W~S side of this volcano and intermittently continuous detonations. The summit area could not be seen owing to clouds, but plume-rising over clouds was confirmed from distance. Before the occurrence of this explosion, increase of volcanic tremors (isolated one, type a or x in Fig. 2-4) and volcanic earthquakes (type S) were detected as seen in Fig. 2-18. Eruptive activities occurred on February 8 and 9, too.

By the explosion on February 7, the characteristic ground vibration was recorded with seismographs at both of stations. The vibrations are not a single explosion-earthquake, but rather seem to be a chain of successive

& various tremors. The vibration has a small amplitude phase in the beginning, then large-amplitude waves and small-amplitude & continuous waves in the latter phase, and the total duration of the vibration is about five minutes. The writer called herewith "Explosion Tremor" for this vibration generated by the explosion, owing to its long duration. Small shocks took place at 02:23, 02:28 and 02:29, but it is not confirmed that they were accompanied by eruptive activities.

The writer read amplitude & period of continuous waves during about 5 minutes of the seismogram obtained with the Ranger type seismograph settled at Cogon. The explosion-tremor has distinguished features in its wave-form divided into six groups, according to characteristics of amplitude (p-p) & period as shown in Table 2-9. The first group (a) is low amplitude, then second (b)

Table 2-9 Mean values of amplitude & period and duration of each phase of the explosion tremor generated by the explosion on February 7, 1980 of volcano Bulusan. (observed at Cogon).

Phase	Amplitude	Period	Duration
	μ	s	s
a	0.20	0.41	16.4
b	0.11	0.38	3.8
c	1.11	0.54	64.7
d	0.51	0.26	52.0
e	0.21	0.45	45.0
f	0.11	0.55	126.5

of small amplitude & short period waves for 3.8 seconds and major wave (c) with large amplitude & rather long period continued for more than one minute. Waves (d) of rather large amplitude & short period continued for about one minute and then small & rather long period waves (e and f) continued. All duration time was about 5.14 minutes.

Mean amplitude (velocity & p-p) and mean period of continuous 10 waves are shown in Fig. 2-19. The lowest alphabetical letters in this figure denote the above-mentioned groups. Mean displacement-amplitude (p-p) & the period are also given in Table 2-10. During occurrence of the explosion, several detonations or intermittent hissing sounds were heard at the skirt of this volcano, for example Irosin, ca. 8 km S of the summit. And the long duration

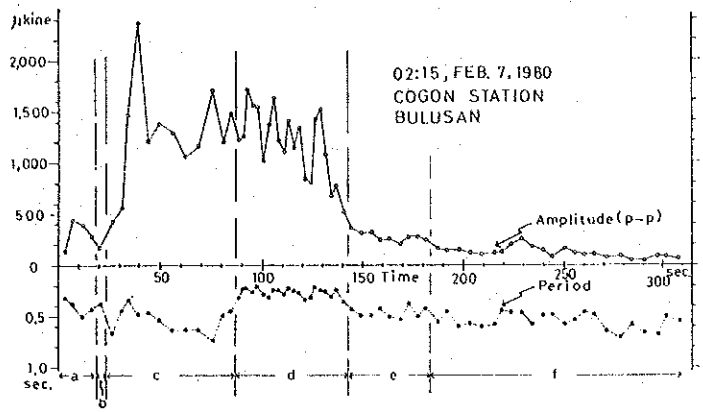

Fig. 2-19 Variation of amplitude and period of continuous 10 waves of the explosion-tremor generated by the explosion on February 7, 1980 at volcano Bulusan.

Table 2-10 Mean amplitude and mean period of continuous 10 waves of the explosion-tremor observed at Cogon by the COMVOL on February 7, 1980 at volcano Bulusan.

Interval	Amplitude	Period	Interval	Amplitude	Period
0.0-3.2 S	0.063 μ	0.32 S	-134.5 S	0.340 μ	0.30 S
-7.0	0.263	0.38	-136.9	0.309	0.24
-12.1	0.309	0.51	-140.4	0.281	0.35
-16.4	0.181	0.43	-144.7	0.240	0.43
-20.2	0.107	0.38	-149.6	0.247	0.49
-26.8	0.455	0.66	-154.5	0.255	0.49
-31.2	0.382	0.44	-158.7	0.160	0.42
-34.6	0.780	0.34	-163.8	0.210	0.51
-39.4	1.886	0.48	-169.0	0.163	0.52
-44.0	0.877	0.46	-172.8	0.157	0.38
-49.4	1.193	0.54	-177.7	0.225	0.49
-55.8	1.372	0.64	-181.9	0.155	0.42
-62.1	1.126	0.63	-187.5	0.150	0.56
-68.4	1.243	0.63	-192.0	0.107	0.45
-75.7	2.060	0.73	-197.9	0.150	0.59
-80.5	0.952	0.48	-203.6	0.119	0.57
-84.9	0.958	0.44	-209.6	0.103	0.60
-88.1	0.653	0.32	-215.4	0.109	0.58
-90.4	0.501	0.23	-219.8	0.085	0.44
-92.6	0.752	0.22	-224.4	0.145	0.46
-95.2	0.621	0.26	-229.0	0.162	0.46
-97.2	0.494	0.20	-234.8	0.187	0.58
-100.1	0.509	0.29	-239.7	0.125	0.49
-103.1	0.691	0.30	-244.5	0.077	0.48
-105.4	0.558	0.23	-250.3	0.160	0.58
-107.7	0.416	0.23	-255.6	0.115	0.53
-110.5	0.552	0.28	-260.2	0.070	0.46
-112.7	0.519	0.22	-265.0	0.081	0.48
-115.2	0.460	0.25	-271.4	0.091	0.64
-117.9	0.520	0.27	-278.4	0.111	0.70
-121.3	0.439	0.34	-284.2	0.057	0.58
-124.5	0.432	0.32	-290.7	0.058	0.65
-126.6	0.453	0.21	-297.4	0.098	0.67
-129.0	0.605	0.24	-302.4	0.065	0.50
-131.5	0.431	0.25	-308.4	0.065	0.55

of the explosion-tremor having several wave groups may represent intermittent occurrence of explosions at the summit crater or craters.

For rough estimation of energy-release by the seismic event of the explosion, the author tried two kinds of convenient estimations as mentioned below.

At first, if we assume the explosion-tremor as a single earthquake, the most convenient method to estimate the energy release is to directly apply the equation to calculate magnitude of tectonic events. In case of Japan, the equation (3) is used by the Japan Meteorological Agency to calculate magnitude of tectonic earthquakes in and around Japan. For usage of the equation, however, we have to ignor fundamental differences of the type of used seismograph, short distance and used component of waves.

$$M = \log A + 1.73 \log D - 0.83 \qquad (3)$$

where A; maximum amplitude (μ) and
D; distance (km)

By using the magnitude by the equation (3), we can get its energy by the equation (4).

$$\log E = 1.5 M + 11.8 \qquad (4)$$

The maximum amplitude and the period of this explosion tremor was 16.4 mm (p-p) & 0.6 sec. on the seismogram, respectively. From displacement magnification at 0.6 sec., the maximum amplitude of 2.22 μ was obtained, and we get magnitude (M) of 0.66 and energy (E) of 6.17×10^{12} erg by equations of (3) & (4).

Then, if we treat "the explosion tremor" on February 7 as volcanic tremor, we can use the equation (5) proposed by Yokoyama (1956)[6] by putting the wave as Rayleigh type waves. And when we use vertical component of volcanic tremor in Rayleigh type waves, we can put the amplitude of vertical component of volcanic tremor as 0.62 A (0.42 A for horizontal component) as described in the equation (5).

$$E = 5.0\, \pi^2 \rho\, r \left(\frac{c}{0.62}\right)^2 \Sigma A^2 \frac{\Delta T}{\tau} \qquad (5)$$

where ρ ; density
r ; distance
c ; wave velocity
A ; amplitude
ΔT ; duration and
τ ; period

If we assume the following values for this estimation in the equation (5), we obtain a convenient equation (6) to get energy-release by volcanic tremor in case of vertical component waves;

where ρ ; 2.0 gr/cm^3
r ; 4.6×10^3 m
c ; 1×10^3m/sec
A ; amplitude of tremor (μ)
ΔT ; duration (sec) and
τ ; period (sec)

$$E = 1.18 \times 10^{10} \Sigma A^2 \frac{\Delta T}{\tau} \quad \text{(erg)} \qquad (6)$$

On the basis of values given in Table 2-10, we can get energy (E) of 7.06×10^{11} erg by the equation (6) and M of 0.03 by the equation (4).

There are large differences between two values, but we can not extend further estimation because of lack of analized materials of horizontal components of waves.

The explosion ejected 6000 m high ash-plume and caused ash-fall in wide area. However, the energy-release of 10^{11} ~ 10^{12} erg or the magnitude less than 0.7 for seismic event accompanied by the explosion does not belong to large energy-release by big explosions. The values belong to examples of small scale explosions of Sakurazima, Kyusyu, Japan. In case of explosions of volcano Sakurazima, magnitude more than 1.0 of explosion-earthquakes (calculated by the equation (3)) are generated by explosions accompanied by ash-plume higher than 3000 m, block-ejections onto the middle flank (1~2 km out of the crater) and rather much quantity of ash-fall around the volcano. Of course, we can not do direct comparison between two cases, owing to differences of used seismographs, distance and components of waves. More detailed invesigations of relation between total mass of ejected materials and magnitude of explosion earthquakes/ tremors are necessary to know the magnitude of volcanic explosions.

§3. Geothermal Inspection

1. Characteristics of Thermometer

(1) Portable Infrared thermometer

One portable Infrared thermometer (IR thermometer) was brought from Japan to operate thermal measurements of surface temperature at volcano Taal. The main specifics of the IR thermometer is as follows;

Type; ER-2002/SD (National Ltd., Japan)
Detector; $PbTiO_2$ pyroelectric infrared detector
Field of view; 0.5°
Sensitivity; narrow; 0.5°C, wide; 1°C
Detective range; narrow; 0° ~ +80°C, wide; -40°~+120°C
Response time: fast; 0.1 sec., slow; 1.0 sec.
Spectrum band pass; 8.5 - 12 μm
Power; Ni-Cd battery, chargeable

We can use this instrument without AC supply for about 8 hours. For charge of the power, 100V AC by a gasolline generator or by a voltage-regulator for 200 V AC was used.

(2) Thermistor thermometer

This thermometer was also brought from Japan to measure ground & water temperature at geothermal areas. The major characteristics is as follows;

Type; A 600-1 (Takara Ltd., Japan)
Sensor; PXA-36, glass thermistor mounted with SUS pipe.
Detective range; low; 0° - 150°C high; 150°-300°C
Sensitivity; 0.2°C
Power; 1.5 V dry cell

2. Operation of Geothermal Inspection and Its Analysis at Volcano Taal

Measurements of surface temperature at high temperature areas with a portable IR thermometer could not be operated during day-time owing to disturbances by high radiation caused by strong sun-shine. So, most of geothermal measurements were conducted under cloudy condition (cloudiness; 9-10) in the mornings. At the conditions, measurements of surface temperatures were not disturbed by the effects of sun-shine and we could detect thermal anomaly of ground surface higher than mean air temperature (average; 28°C).

Measurements in fields were mainly operated by the following convenient method. First, the objective site was decided and the photographs of the site were taken by a polaroid camera. All of measurement points were plotted in the pictures with numerical number and measurements of surface-temperature at the points were carried out by panning & tilting of the IR thermometer fixed on a tripole with manual operations.

After geographical correction for inclined slopes of measurement sites, distribution of surface temperatures are plotted & illustrated in a map and then areas of isothermal range are obtained. To estimate heat-flux by results of surface-temperature has been developped by Sekioka & Yuhara (1974)[7] in case of steaming ground by the equation (7).

$$\Delta Q = e(1-0.09m)(0.52+0.065\sqrt{e_w})\sigma\Delta T_0^4 + \rho_a C_p D(1+r)\Delta\theta_0 \qquad (7)$$

where ΔQ ; difference between geothermal flux
e ; emissivity
m ; cloudiness
e_w ; vapour pressure
T_0 ; surface temperature (°K)
ρ_a ; air density
D ; transfer velocity
r ; reciprocal of Bowen ratio
θ_0 ; surface temperature (°C)
σ ; Stefan-Boltzman's constant and
C_p ; specific heat of air at constant pressure

The author estimated the heat-flux out of volcano Taal based on measuremets of surface-temperatures under the following assumptions in the equation (7).

$e = 1.0$
$m = 10$
$e_w = 37.8$ mb (at 28°C)
$\Delta T_0^4 \fallingdotseq 8.14 \times 10^7 \Delta\theta_0$ °C
$\rho_a = 1.1 \times 10^{-3}$ g/cm^3
$D = 3.5$ cm^2/s
$r = 0.06$
$\sigma = 1.36 \times 10^{-12}$ cal cm^{-2}K^{-4}s^{-1} and
$C_p = 0.239$ cal g^{-1}K^{-1}

By using the above-mentioned values, the following convenient equation (8) is obtained to estimate heat flux in case of ordinary surface temperature of 28°C for analysis at volcano Taal.

$$\Delta Q = 9.8 \times 10^{-4}\ \Delta\theta\Delta S \qquad \text{(cal/sec)} \qquad (8)$$

where $\Delta\theta$; difference between surface temperatures of geothermal anomaly and non-geothermal ground. (°C) and

ΔS ; area showing same surface-temperature (cm^2)

By this equation, we can obtain difference between two geothermal heat-flux by the difference of surface temperatures among two sites. So, we can estimate total heat-flux at volcano Taal with the equation (8) from various areas of isothermal distribution at available intervals.

There, however, are not only steaming ground but also vapour risings at high temperature areas such as the New Eruption Site. In case of plume rising, we can use the following equation (9) proposed by Briggs (1969) [8]

$$Q = 2.6 \times 10^{4}\ u^{3}\ h^{3}\ x^{-2} \qquad \text{(cal/sec)} \qquad (9)$$

where u ; wind velocity (m/sec)

h ; height of fume (m) and

x ; lateral distance from heat-source (m)

If we can get exact wind speed at a height of plume rising, the equation is very convenient to estimate heat-flux of plume, but usually we can not reject big accidental error in this method without detailed materials.

3. Distribution of High Temperature Areas at Volcano Taal

During the Research Work at volcano Taal, average value of the lowest air-temperature in the mornings under cloudy condition was about 28°C. So, inside this volcano, the author selected high temperature areas which show the surface-temperature higher than 28°C as geothermal anomalies.

Not only surface temperature, but also underground temperature was also measured with the thermistor thermometer to detect thermal anomaly in ground or water. The major positions where thermal inspections were operated are

shown in Fig. 3-1 by open circles. Dotted arrows denote directions of thermal measurements with the IR thermometer across the Main Crater lake. (Solid circles denote seismological inspection-points).

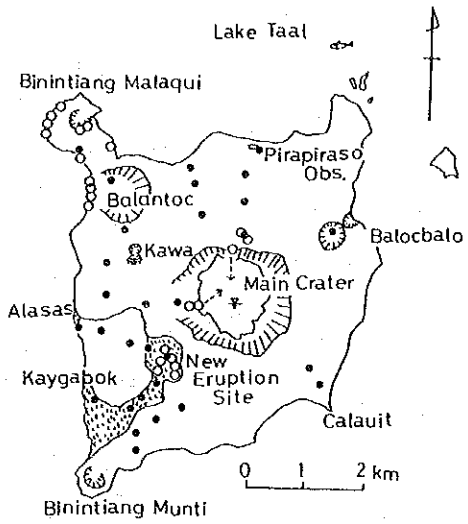

Fig. 3-1 Measurement sites for geothermal inspection (open circle) during this research work at volcano Taal. Solid circle denotes seismological inspection point.

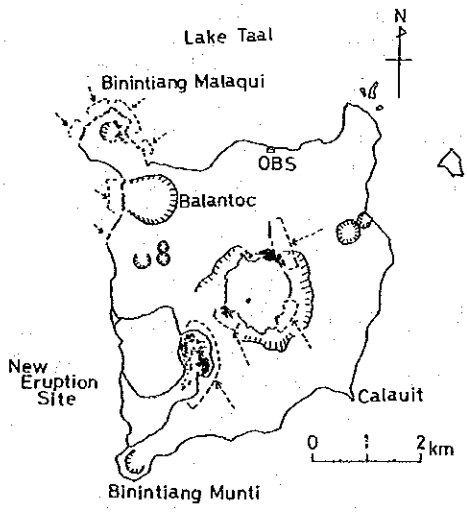

Fig. 3-2 Distribution of geothermal anomaly of ground surface inside Taal volcano island detected with this thermal inspections (January, 1980).

The distribution of geothermal anomaly areas showing high temperatures detected by this research work is illustrated with solid patches with dotted arrows in Fig. 3-2. The distributions are clear around B. Malaqui, the lake shore of Mt. Balantoc, at the northern slope of Main Crater, the N, SW & SE parts of the inner wall of Main Crater, and craters & lava-flow at the New Eruption Site.

There was no remarkable geothermal anomaly on the surface of Main Crater lake and no discoloration on the surface of lake water. Almost of high temperature areas show discolored solfataric fields without grass or plants. There were not any discolorations of water at site of hot-water and not spoutings of hot-water along the lake-shore of B. Malaqui & Mt. Balantoc.

From Fig. 3-2, we can see that high temperature areas do not distribute at the eastern side and are remerkable around the central part of this volcano island and around B. Malaqui. We also see a rough linear or zonal distribution of high temperature areas in the direction of NE- SW bonding the northern part of Main Crater through the New Eruption Site. In case of the 1965 Explosion, a direction of NE-SW arrangement of opened craters by fissure was clear and there is also a linear distribution of new craters such as 1976 and 1977 cones in the present New Eruption Site (ca. N-35°~40° -E).

This linear distribution of high temperature areas bonding Main Crater and the New Eruption Site will represent the underground tectonic structure developped at this volcano.

4. Isothermal Distribution in High Temperature Areas at Volcano Taal

To estimate heat-flux out of volcano Taal, first we have to know precise distribution of surface temperature in respective geothermal anomaly sites. Fig. 3-3 is an example of thermal distribution inside a small high temperature patch on the SE rim of B. Malaqui measured with the thermistor thermometer at the depth of 10 cm. A sharp distribution of high temperature higher than 70°C is detected inside the patch with spot-measurements by a thermistor probe, but we get mean distributions of surface temperature in case of measurements with the IR thermometer.

In Fig. 3-4~3-7, isothermal distribution of surface temperature higher than 28°C at Main Crater, 1976 Crater and the Elongated Crater are shown.

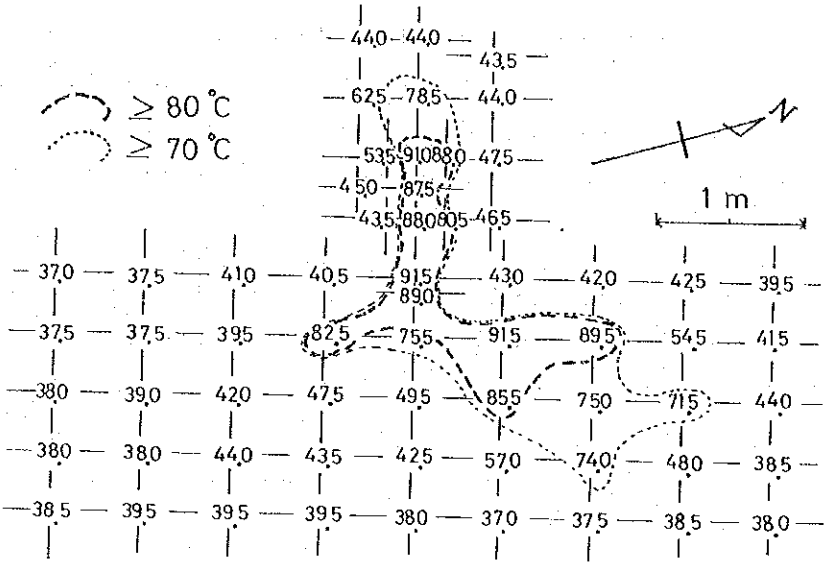

Fig. 3-3 10-cm deep ground temperature in a high temperature patch on the SE rim of B. Malaqui Crater (January 25, 1980).

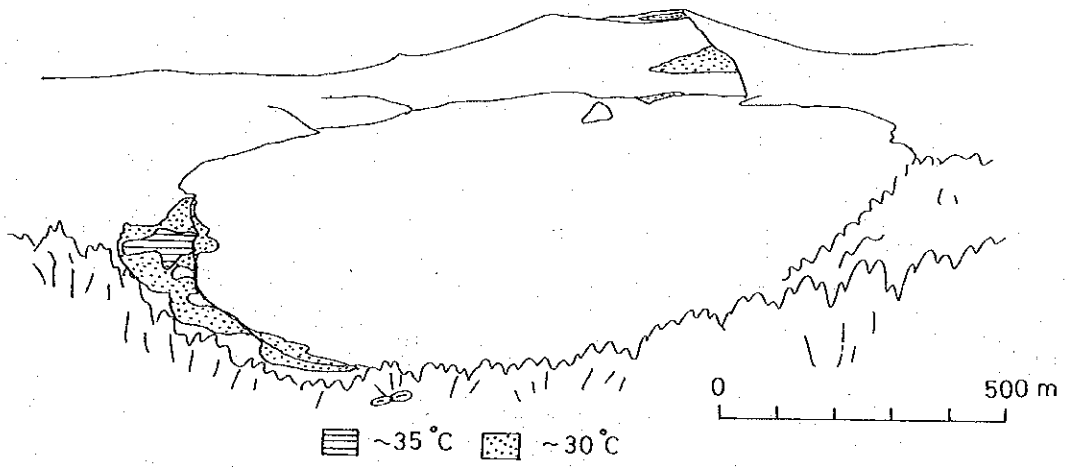

Fig. 3-4 Isothermal distribution detected at the N side of Main Crater on January 18, 1980.

Fig. 3-4 is a distribution of geothermal anomaly around the Main Crater measured at the N rim of Main Crater, and a thermal distribution measured at the SW side is in Fig. 3-5. From these measurements, high surface temperatures more than 40°C were detected at the north inner crater-wall.

Fig. 3-6 is a geothermal distribution of ground surface of 1976 Crater in the New Eruption Site. We detected the remarkable thermal anomaly more

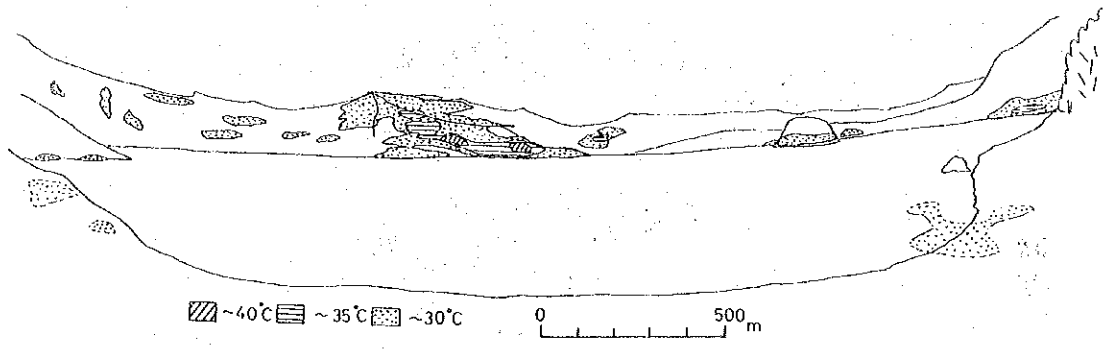

Fig. 3-5 Isothermal distribution of the inner of Main Crater detected at the SW shore of the crater lake on January 27, 1980.

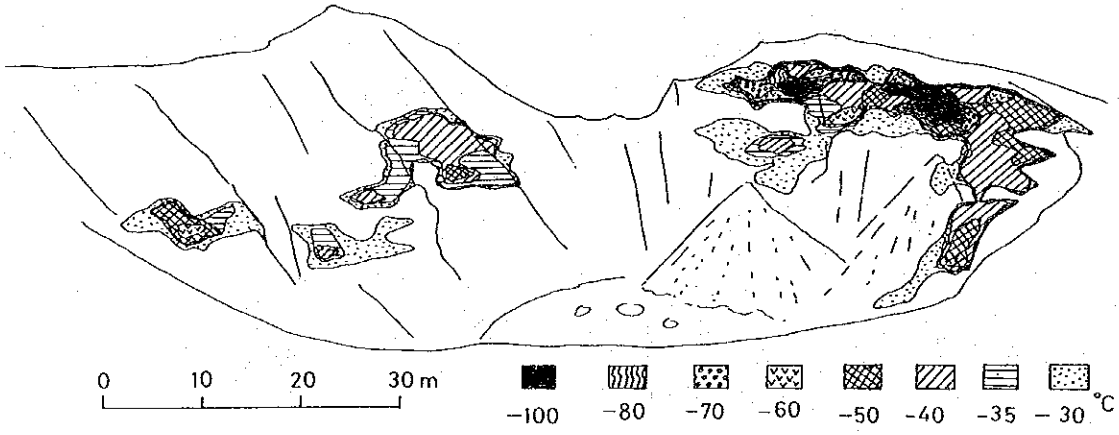

Fig. 3-6 Isothermal distribution inside 1976 Crater at the New Eruption Site detected at its NE side on January 18, 1980.

than 100°C at the northern upper part of the inner crater-wall of this crater as shown in this figure. But, we did not any geothermal anomaly on the crater-bottom. At this crater, the activest vapour-rising of this volcano is seen at the site where shows high temperature more than 100°C.

Rising of vapour is seen only around the New Eruption Site, but not so strong except 1976 Crater. The brief of vapour-rising is given in Table 3-1.

Fig. 3-7 is a geothermal distribution of ground-surface inside the Elongated Crater which has a small cone formed in 1977 at the NE side of the crater-bottom. There are seen two high temperature areas more than higher 60°C in this figure, but the right is the highest site of 1976 Crater. Vapour-rising at this crater was weak.

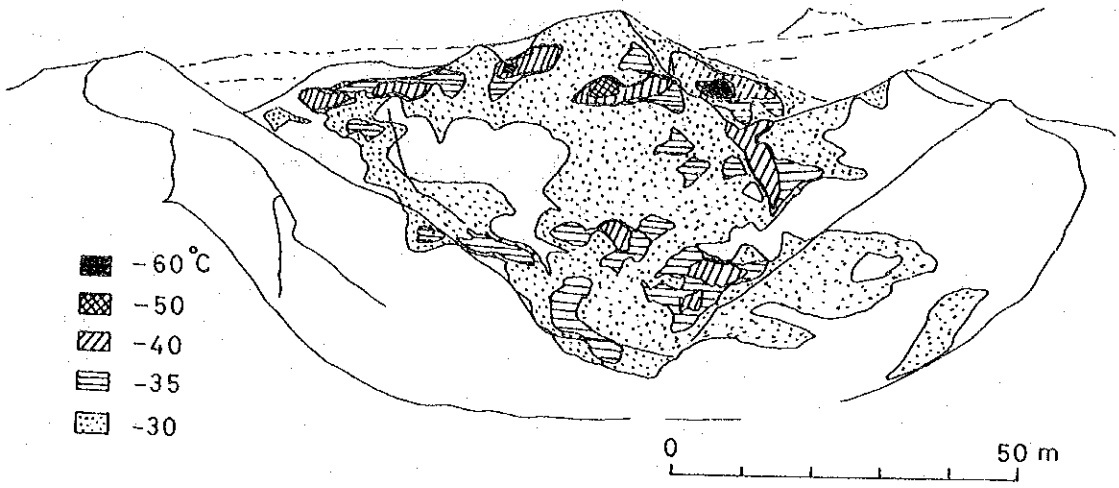

Fig. 3-7 Isothermal distribution inside the Elongated Crater at the New Eruption Site detected at the NE rim of the crater on January 23, 1980. The highest area at the right side in this figure represents the one in 1976 Crater.

Table 3-1 Observational data of fume rise at the New Eruption Site, volcano Taal on January 18, 1980.

Location	Color	Quantity	Height (m)
North side of 1976 Crater	white	medium	30-50
Collapsed Crater	white	small	5-10
1969 Lava Flow	white	small	2-5
Elongated Crater	white	small	2-5

No fizzing sound

5. Estimaiton of Heat Flux at Volcano Taal

The author tried to estimate total amount of heat-flux based on observed surface-temperatures at geothermal anomaly areas and by the method developped by Sekioka & Yuhara (1974)[7]. Mean temperature, difference of temperature ($\Delta\theta$), areas of isothermal distribution and heat-flux at each isothermal area are given in Table 3-2. Heat-flux at the major high temperature areas are also given in Table 3-3.

Table 3-2 Heat discharge and area of isothermal part in high temperature areas at volcano Taal.

Mean Temperature	Δθ	Area	Heat Flux
°C	°C	cm^2	cal/sec
Main Crater			
30.4	2.4	7.43×10^8	1.75×10^6
30.5	2.5	0.97×10^8	0.24×10^6
37.2	9.2	0.45×10^8	0.41×10^6
37.7	9.7	0.43×10^7	0.41×10^5
41.5	13.5	0.42×10^7	0.56×10^5
42.0	14.0	0.07×10^7	0.96×10^4
total		8.94×10^8	2.50×10^6
Northern Slope			
37.0	9.0	0.70×10^6	0.62×10^4
40.0	12.0	1.80×10^6	2.12×10^4
45.0	17.0	3.69×10^6	6.15×10^4
total		6.19×10^6	0.89×10^5
New Eruption Site			
(1)1976 Cone			
30.8	2.8	3.28×10^5	0.90×10^3
36.3	8.3	1.05×10^5	0.85×10^3
42.5	14.5	0.15×10^5	0.22×10^3
48.5	20.5	0.11×10^5	0.22×10^3
53.2	25.2	0.83×10^4	0.21×10^3
56.8	28.8	0.51×10^4	0.14×10^3
67.0	39.0	0.16×10^4	0.06×10^3
72.7	44.7	0.34×10^4	0.15×10^3
total		4.77×10^5	2.75×10^3
(2)Solfatara near Collapsed Crater			
30.6	2.6	5.05×10^5	1.29×10^3
36.8	8.8	0.11×10^5	0.95×10^2
42.2	14.2	0.73×10^4	1.02×10^2
46.0	18.0	0.12×10^4	0.21×10^2
52.0	24.0	0.94×10^3	0.22×10^2
59.0	31.0	1.56×10^3	0.47×10^2
69.0	41.0	0.62×10^3	0.25×10^2
total		5.28×10^5	1.60×10^3
(3)Collapsed Crater			
31.3	3.3	0.99×10^6	3.20×10^3
36.0	8.0	0.21×10^5	0.16×10^3
42.0	14.0	1.01×10^5	1.39×10^3
51.0	23.0	0.13×10^5	0.29×10^3
total		1.13×10^6	5.05×10^3
(4)1976 Crater			
30.5	2.5	1.58×10^6	0.39×10^4
37.3	9.3	0.29×10^6	0.26×10^4
41.8	13.8	0.39×10^6	0.53×10^4
48.0	20.0	0.59×10^6	1.16×10^4
56.2	28.2	0.72×10^5	0.20×10^4
62.3	34.3	0.67×10^5	0.22×10^4
66.5	38.5	0.47×10^5	0.18×10^4
72.0	44.0	0.18×10^5	0.78×10^3
77.3	49.3	0.35×10^5	1.69×10^3
85.0	57.0	0.18×10^5	1.01×10^3
100.0	72.0	0.67×10^4	0.47×10^3
107.0	79.0	1.33×10^4	1.03×10^3
114.0	86.0	1.89×10^4	1.59×10^3
117.0	89.0	0.89×10^4	0.78×10^3
total		3.15×10^6	3.67×10^4

Table 3-2 (Continued)

Mean Temperature	Δθ	Area	Heat Flux
°C	°C	cm^2	cal/sec
(5)Elongated Crater			
31.0	3.0	1.97×10^7	5.79×10^4
36.7	8.7	0.75×10^6	0.64×10^4
41.9	13.9	0.30×10^6	0.41×10^4
46.3	18.3	0.86×10^5	0.15×10^4
51.0	23.0	0.11×10^5	0.25×10^3
67.0	39.0	0.08×10^5	0.31×10^3
total		2.09×10^7	7.05×10^4
Total((1)-(5))		2.62×10^7	1.17×10^5
1969 Lava Flow			
35.0	7.0	2.00×10^5	1.37×10^3
35.3	7.3	0.50×10^4	0.36×10^2
36.0	8.0	0.20×10^5	0.16×10^3
38.0	10.0	0.50×10^5	0.49×10^3
40.0	12.0	9.75×10^5	1.15×10^4
41.0	13.0	1.76×10^3	0.22×10^2
43.0	15.0	1.71×10^6	0.25×10^5
48.0	20.0	0.90×10^5	1.76×10^3
49.0	21.0	0.64×10^3	0.13×10^2
50.0	22.0	9.45×10^5	2.04×10^4
52.0	24.0	4.38×10^5	1.03×10^4
55.0	27.0	4.50×10^4	1.19×10^3
56.0	28.0	0.20×10^5	0.55×10^3
60.0	32.0	0.20×10^5	0.63×10^3
62.0	34.0	1.04×10^6	3.47×10^4
65.0	37.0	1.30×10^5	4.71×10^3
68.0	40.0	1.40×10^5	0.55×10^4
72.0	44.0	0.74×10^3	0.32×10^2
74.0	46.0	2.04×10^5	9.20×10^3
76.1	48.1	0.91×10^5	0.43×10^4
78.0	50.0	1.50×10^5	7.35×10^3
80.0	52.0	3.20×10^2	0.16×10^2
83.0	55.0	0.40×10^5	2.16×10^3
85.0	57.0	1.01×10^5	5.64×10^3
90.0	62.0	0.50×10^4	0.30×10^3
94.0	66.0	0.10×10^5	0.65×10^3
96.0	68.0	1.18×10^3	0.79×10^2
120.0	92.0	3.04×10^2	0.27×10^2
125.0	97.0	0.86×10^3	0.82×10^2
151.0	123.0	0.71×10^3	0.86×10^2
total		6.44×10^6	1.48×10^5
B.Malaqui (*; shore)			
40.0	12.0	4.23×10^6	0.50×10^5
50.0	22.0	1.21×10^6	0.26×10^5
60.0	32.0	0.60×10^6	0.19×10^5
42.5*	14.5	1.26×10^7	1.79×10^5
total		1.86×10^7	2.74×10^5
Mt. Balantoc			
40.0	12.0	0.40×10^6	0.47×10^4
45.0	17.0	0.60×10^7	1.00×10^5
50.0	22.0	0.20×10^6	0.43×10^4
55.0	27.0	0.20×10^6	0.53×10^4
60.0	32.0	0.20×10^5	0.63×10^3
total		6.82×10^6	1.15×10^5

From Table 3-3, we can see that the largest heat-discharge is detected at Main Crater and the second at B. Malaqui. The former represents existence of wide areas of geothermal anomaly and the latter not only wide areas of geothermal anomaly at the crater rim, but also wide distribution of high temperatures around the shore.

Table 3-3 Heat discharge at the major geothermal areas at volcano Taal.

Location	Area	Heat Flux
Main Crater	8.94×10^8 cm^2	2.50×10^6 cal / sec
Northern Slope	6.19×10^6	0.89×10^5
New Eruption Site	2.62×10^7	1.17×10^5
Lava Flow	6.44×10^6	1.48×10^5
B. Malaqui	1.86×10^7	2.74×10^5
Mt. Balantoc	6.82×10^6	1.15×10^5
Total	9.58×10^8	3.24×10^6

The total heat-flux out of this volcano was estimated as 3.24×10^6 cal/sec. From plume rising at 1976 Crater, a rough estimation was tried, too, by using the following values in the equation (9); 40 m for height of plume (h), 20 m for lateral distance (x) from heat source and 2 m/sec for wind-velocity (u). Then we get heat-flux of 3.33×10^7 cal/sec. The estimation has to be corrected by more detailed/precise measurements of meteorological condition at respective altitude and of rising-rate of plume.

When we directly compare the heat-flux estimated here to the values of active volcanoes in Japan obtained by Kagiyama (1978) [9], we see that the value of heat-flux of 3.33×10^7 cal/sec are around ones out of Oosima in 1976, Nasu, Usu (Syowa-Sinzan), Akan and Kirisima which show active plume-risings. The heat-flux of 3.24×10^6 cal/sec also belongs to ones of active geothermal anomaly in case of active volcanoes in Japan. So, we consider that volcano Taal is very active from geothermal viewpoint of volcanic activity.

6. Geothermal Anomaly Detected by Airborne Infrared Scanner

Infrared Images of volcano Taal by airborne IR scanner have been taken in 1965 and 1966 [10], [11]. The auther could see the geothermal anomaly inside volcano Taal in 1965 as white spots in black & white pictures of IR images and compare the results obtained by this research. It is difficult to compare

each surface-temperature between the two results because of lack of gray-scales in the IR images. The geothermal anomalies in IR images taken in 1965 are shown by black spots with broken arrows in Fig. 3-8. A and B in this figure mean the areas of B. Malaqui and Main Crater, respectively.

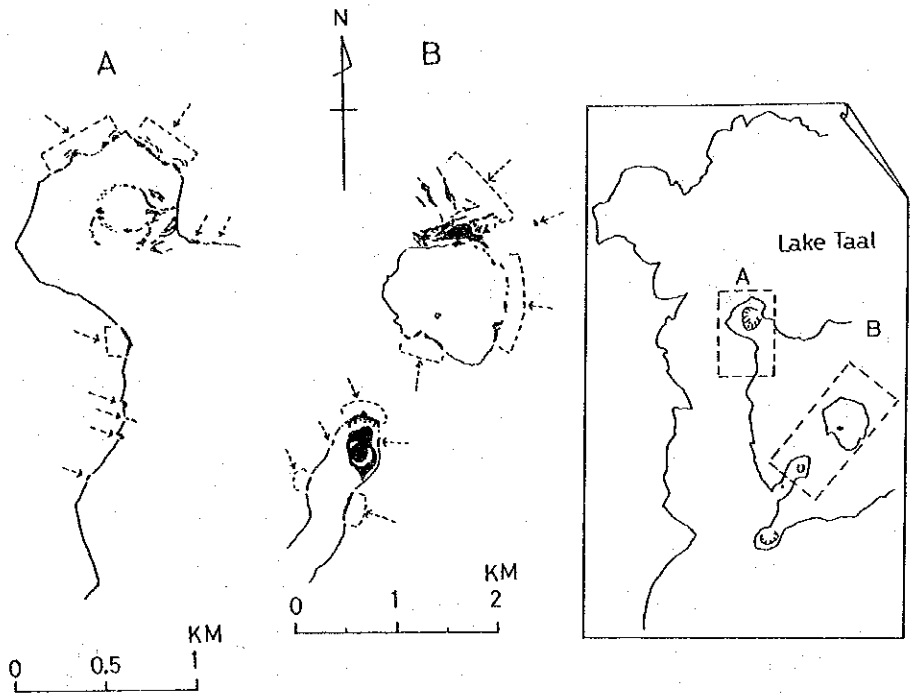

Fig. 3-8 Distribution of thermal anomaly inside Taal volcano island detected in Infrared images taken by airborne Infrared scanner in 1965 [10], [11].

The locations of geothermal anomaly in 1965 inside this volcano island are almost same as the result obtained by this research work, excepting the remarkable geographical change at the SE side, of lagoon formed by the 1965 strong explosions. The area has been burried with a large amount of the 1968 & 1969 lava flows and new cones, and is now called the New Eruption Site which shows the activest geothermal anomaly in & around new craters and in lava flows.

We are able to do rough comparison of the width of areas of geothermal anomaly among the results by IR images in 1965 and the results by this research work. We see that the geothermal anomaly at B. Malaqui and around Main Crater in 1965 are rather wider than those in 1980. Decreasing of water-temperature of Main Crater after the 1965 Explosion has been confirmed

by thermal measurements by the COMVOL, and decreasings of ground-temperature of fumaroles in the New Eruption Site, of geothermal areas around B. Malaqui and around Main Crater have been confirmed in recent years by periodical measurements by Pirapiraso Observatory.

We can conclude that there are still active geothermal anomaly and high heat-discharge at volcano Taal, but the geothermal activity seem to be in rather low comparing the state in 1965. Geothermal activity of this volcano may gradually decrease in recent years. Periodical & systematic aerial IR inspections are very effective for monitoring of geothermal anomalies of active volcanoes.

7. Hot Spring at the Foot of Volcano Bulusan

Remarkable variation of water temperature of hot spring at San Benon has been detected in case of the 1978 Euption of this volcano[12]. We checked and measured water-temperatures of two hot springs at San Benon and Masacrot, San Roque. The locations are given in Fig. 2-17.

After beginning of volcanic eruptions since the end of 1979, no remarkable changes of water temperature of hot spring at San Benon was detected by the periodical measurements by the COMVOL. There was no any extra-ordinary state at hot springs at Masacrot, too.

Hot water of both hot springs is none colored and there were not fumarolic activities around hot springs. Water temperature by our measurement is shown in Table 3-4. In this table, water temperature of the surface of Lake Bulusan is also given for information.

Table 3-4 Water temperatures of two hot springs and Lake Bulusan with the portable Infrared thermometer at volcano Bulusan.

Location	Date	Water Temperature
San Benon Hot Spring		
No. 1	Feb. 10, 1980	44 °C
	"	47
	"	37
No. 2	"	37
Masacrot Hot Spring	Feb. 11, 1980	35
	"	34
	"	25*
Lake Bulusan**	Feb. 11, 1980	22-23

* ground temperature at 10 cm depth, near spring

** surface of lake-water

§4. Magnetic Inspection

COMVOL has been executing the repetition of the magentic survey in the total intensity by mean of proton precession magnetometer on Taal and Mayon volcano for the purpose of the ditection of volcanomagnetic effects.[13),(14),(15)]

On this joint research work, observation of magnetic distribution was made on and around Taal volcano and some experimental observations to detect volcanomagnetic effects were done on Taal, Bulusan and Mayon volcano using a proton precession magnetometer. This magnetometer, which was carried from Japan, is a manual opration type (PPM-739B, Sokkisha ltd., Japan) and it's resolution is 1 nT (gamma).

1. Magnetic property of rock samples on Taal volcano

Basaltic lava flow in 1969 and old lava flow are exposed in the south-western part and in the north-eastern coast of the volcano island respectively. On the purpose of examination of magnetic properties of these lava flows, some rock samples were taken from these lava flows and another. Locations of the sampling sites are shown in Fig. 4-1.

The magnetic properties of the rock samples were examined by Dr. T. Nakatani of the Kono Laboratory, Faculty of Science, the University of Tokyo. The sample were devided into small specimens and the properties were investigated for each specimen. Table 4-1 shows the natural remanent magnetization (NRM) and the susceptibility (κ) with mean values. Rock samples S1, S2, and S6 were taken from the 1969 lava flow, S3 and S4 were done from the old lava flow. S5 is a porous material which is considered to be erupted.

The NRM is nearly magnetized in the direction of the present magnetic field except for the samples S2 and S5. The average intensity of the NRM of the 1969 lava flow is about 5×10^{-2} emu/cc and it's Konigsberger ratio Q, which is the ratio of NRM to induced magnetization, ranges from 34 to 230. On the old lava, the average intensity of the NRM is about 1×10^{-2} emu/cc and Q is about 5.

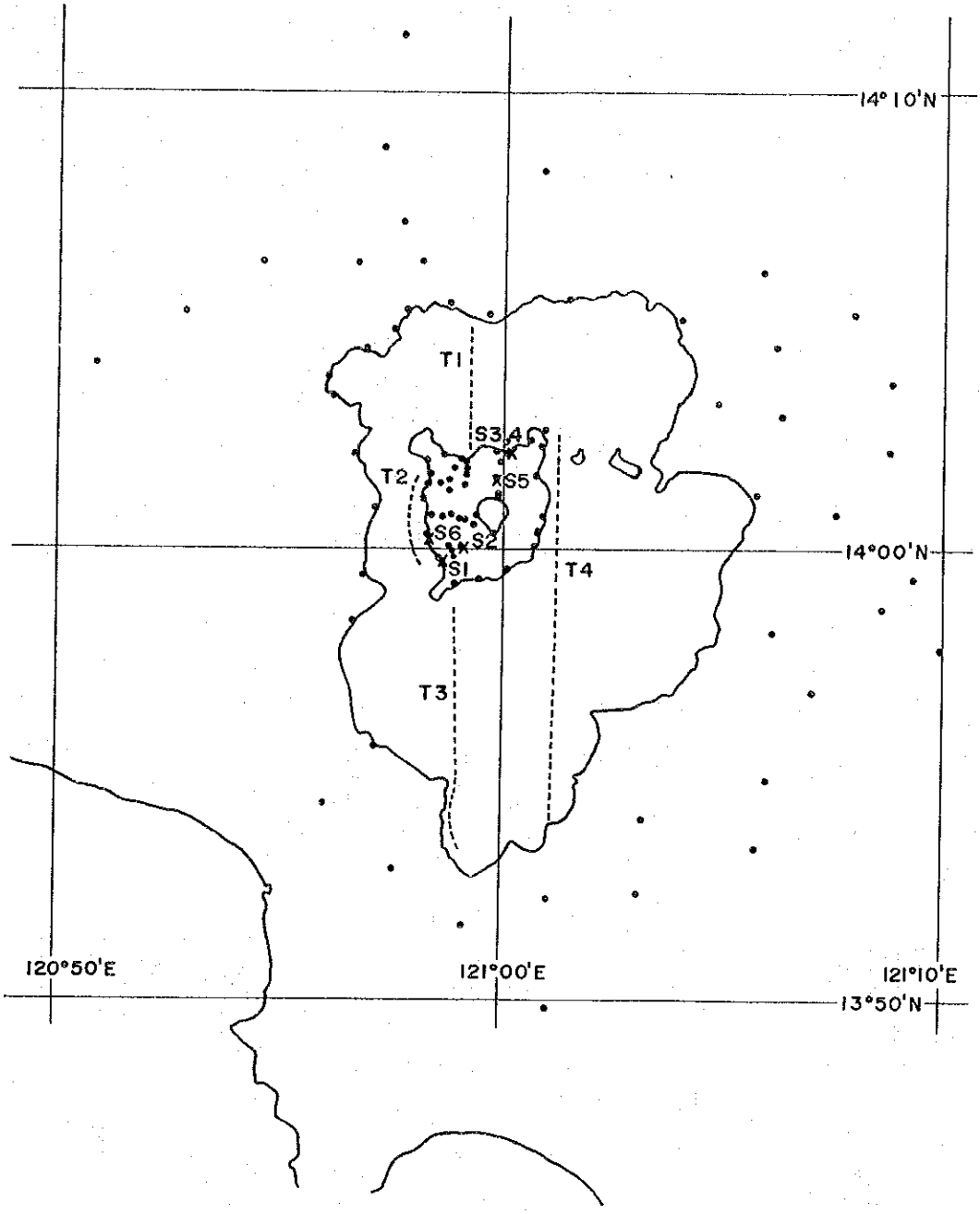

Fig. 4-1 Map showing the distribution of geomagnetic observation points (solid circles) and tracks (broken lines). Crosses indicate locations of rock sampling.

Table 4-1 Natural remanent magnetization and susceptibility of rock samples on Taal volcano.

Sample	Natural Remanent Magnetization (NRM)				Susceptibility (K)
	Intensity		Dip	Dec.	
	emu/gr.	emu/cc	deg.	deg.	emu/gr.
S1	2.69×10^{-2}	5.66×10^{-2}	31.8	-9.1	3.63×10^{-4}
S2	1.89×10^{-2}	4.19×10^{-3}	30.3	-164.1	1.10×10^{-3}
S3	6.31×10^{-3}	1.34×10^{-2}	20.5	-16.4	3.72×10^{-3}
S4	6.14×10^{-3}	9.65×10^{-3}	34.1	-25.0	3.01×10^{-3}
S5	7.75×10^{-4}	1.00×10^{-3}	-0.5	93.2	3.22×10^{-3}
S6	2.47×10^{-2}	5.52×10^{-2}	13.7	-5.7	3.93×10^{-3}

2. Diurnal variation of the geomagnetic total intensity

As Philippine islands are situated near the magnetic dip equator, the diurnal variations are considerably afffected by the equatorial jet current in the ionosphere.

In the case of customary magnetic survey, variations of geomagnetic field are continuously recorded at a base station near magnetic survey area in order to estimate general magnetic disturbances such as diurnal variation, magnetic storm and like. But in such a case that, only one magnetometer is used for magenetic inspection, observed values at a standard magnetic observatory which is not so far from the inspection area are needed to eliminate non-local geomagnetic variations.

In Philippines, there is a standard magnetic observatory at Muntinlupa which is belong to BCGS (Bureau of Coast & Geodetic Survey) and is situated at lat. 14°22'24.8" N and long. 121°00'57.1" E.

In order to estimate the accuracy of eliminating of non-local geomagn-

Table 4-2 Geomagnetic total intensity at Pirapiraso

Date	Time (LT)	Observed Value	Date	Time (LT)	Observed Value	Date	Time (LT)	Observed Value
1980	h m	nT	1980	h m	nT	1980	h m	nT
Jan. 24	14 0	40458.5	Jan. 25	0 0	40416.0	Jan. 25	10 40	40441.0
	10	454.5		10	414.5		50	440.0
	20	453.0		20	414.5		11 0	436.5
	30	450.0		30	414.0		10	435.0
	40	445.5		40	414.0		20	437.0
	45	444.5		50	412.5		30	440.5
	50	444.0		1 0	412.5		40	442.0
	55	442.0		10	412.5		50	444.0
	15 0	440.5		20	415.0		12 0	448.0
	5	441.5		30	417.0		10	448.5
	10	440.0		40	419.5		20	449.0
	15	438.5		50	423.0		30	450.0
	20	439.0		2 0	424.5		40	450.5
	25	438.5		10	424.5		50	451.0
	30	438.0		20	422.0		13 0	450.5
	35	438.0		30	419.5		10	449.0
	40	439.0		40	420.0		20	448.0
	45	438.0		50	419.0		30	447.0
	50	437.0		3 0	418.0		40	448.5
	55	436.5		10	418.0		50	449.0
	16 0	438.0		20	418.0		14 0	447.5
	5	436.5		30	420.0		10	452.5
	10	433.0		40	421.0		20	446.5
	15	435.5		50	422.0		30	446.0
	20	436.0		4 0	421.5		40	445.5
	25	436.0		10	421.5		50	441.5
	30	435.0		20	422.5		15 0	439.0
	35	435.5		30	422.5		10	440.0
	40	436.0		40	423.5		20	436.5
	45	436.5		50	423.5		30	437.0
	50	436.0		5 0	424.5		40	439.0
	19 30	428.0		10	425.0		50	435.0
	40	427.5		20	424.0		16 0	436.5
	50	427.5		30	425.5		10	435.5
	20 0	427.0		40	425.0		15	434.0
	10	423.5		50	424.5		20	437.0
	20	423.5		6 0	423.5		25	441.0
	30	422.5		10	426.5		30	439.5
	40	423.5		20	426.0		35	438.0
	50	424.5		30	425.0		40	438.0
	21 0	426.0		40	425.0		45	437.5
	10	426.5		50	422.5		50	437.0
	20	425.0		7 0	424.5		55	439.0
	30	427.5		10	423.0		17 0	438.5
	40	426.0		20	423.0		5	438.0
	50	426.0		30	424.0		10	440.5
	22 0	423.0		40	426.0		15	439.0
	10	420.0		50	427.5		20	439.5
	20	421.0		8 0	427.0		25	439.0
	25	421.5		10	429.0		30	439.5
	30	420.0		20	431.5		35	438.0
	40	420.0		30	430.5		41	438.0
	45	420.0		40	432.0		50	437.5
	50	419.0		50	434.0		18 0	438.0
	55	419.0		9 0	435.5		10	439.0
	23 0	419.0		10	438.0		20	439.0
	5	416.5		20	439.0		30	441.0
	10	417.0		30	438.5		40	439.5
	15	416.0		40	440.5		50	437.0
	20	416.0		50	443.5		19 0	437.5
	25	416.5		10 0	444.5		10	443.5
	30	416.0		10	445.0		20	450.0
	40	415.5		20	443.0		30	449.0
	50	415.5		30	445.0			

Table 4-3 Geomagnetic total intensity at San Benon

Date	Time (LT)	Observed Value	Date	Time (LT)	Observed Value
1980	h m	nT	1980	h m	nT
Feb. 10	5 20	40009.0	Feb. 10	13 40	40047.0
	25	008.5		50	043.0
	30	009.5		14 0	042.5
	40	009.5		10	039.5
	50	011.0		20	039.0
	6 0	013.0		30	039.5
	10	013.0		40	037.0
	20	014.5		50	035.0
	30	020.0		15 0	032.0
	40	022.0		10	029.0
	50	025.0		20	026.5
	7 0	025.0		30	024.5
	10	026.5		40	023.5
	20	029.5		50	022.5
	23	030.5		16 0	022.0
	40	032.0		10	021.0
	50	036.5		20	021.0
	8 0	039.5		30	021.0
	10	045.0		40	021.0
	20	048.0		50	022.0
	30	051.0		17 0	022.0
	40	056.0		10	023.5
	50	062.5		20	025.0
	9 0	060.5		30	026.0
	10	067.0		40	025.5
	20	073.5		50	025.5
	30	075.5		18 0	027.0
	40	077.5		10	024.0
	50	080.0		20	023.0
	10 0	080.5		30	022.0
	10	085.5		40	023.0
	20	086.5		50	023.0
	30	088.0		19 0	021.0
	40	088.5		10	021.0
	50	087.0		20	020.0
	11 0	086.0		32	019.0
	10	087.0		40	018.5
	20	092.0		50	018.0
	30	091.5		20 0	018.0
	40	085.0		10	017.5
	50	085.0		20	018.0
	12 0	082.0		30	018.0
	5	084.0		40	017.0
	10	085.0		50	016.0
	17	084.0		21 0	016.5
	34	082.0		10	017.0
	40	081.0		20	016.0
	50	076.0		30	016.0
	13 0	066.0		40	015.5
	10	071.0		50	015.0
	20	062.0		22 0	014.5
	30	052.0			

etic variations, the diurnal variations were observed at Taal and Bulusan volcano. The two times measurements in the total intensity were made for ten minute interval on January 24 and 25 at Pirapiraso (Taal volcano) and

on Feburary 10 at San Benon (Bulusan volcano). The mean values of two times measurements are tabulated in Table 4-2 and 4-3 for each station. The diurnal variations at each station and at Muntinlupa Magnetic Observatory are plotted in Fig. 4-2 and 4-3. The differential fields are also shown in the same figures. The total intensity at Muntinlupa was calculated from the value of the horizontal and vertical intensity recorded on the ordinary magnetogram.

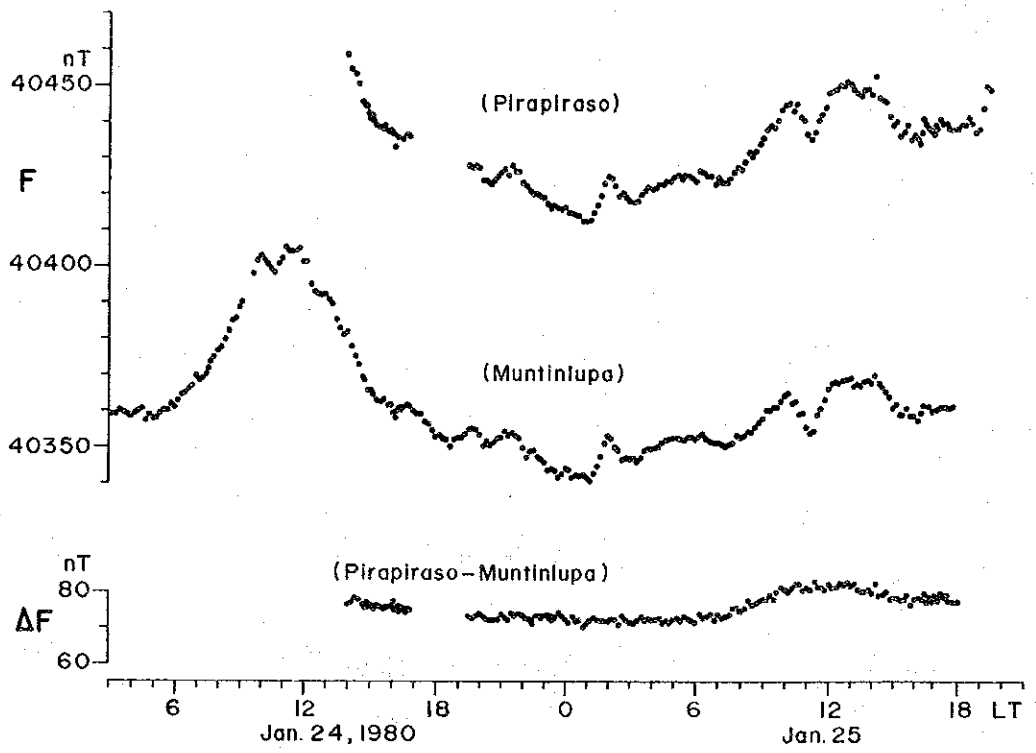

Fig. 4-2 Diurnal variations of the geomagnetic total intensity observed on Jan. 24 and 25, 1980.

Although the diurnal variation on January 25 was unusual, the diurnal viriation in the differencial field between Pirapiraso and Muntinlupa was estimated to be about 10 nT. While, the differencial field between San Benon and Muntinlupa scattered than the above. As short period geomagnetic disturbances occured during the observation period, the scattering are considered to be caused mostly by the difference in the condition of underground electrical conductivities.

As the results, the errour of eliminating non-local changes was estimated as ± 5 nT at Taal area and as ± 10 nT at Bulusan area.

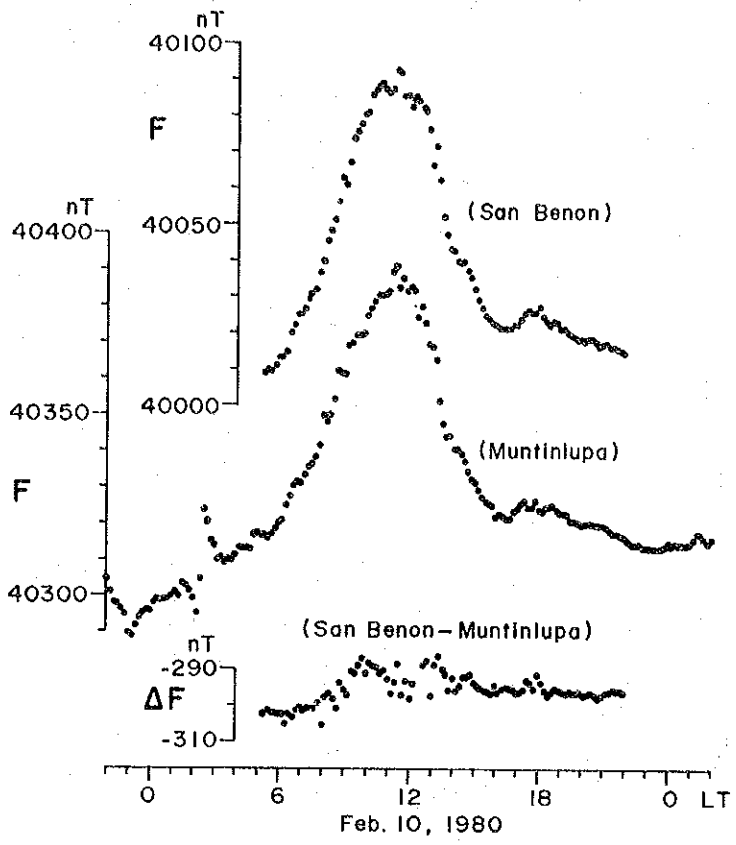

Fig. 4-3 Diurnal variations of the geomagnetic total intensity observed on Feb. 10, 1980.

3. Magnetic survey on and around Taal volcano

Magnetic survey was carried out in order to search the subterranean structure of Taal volcano.

Observations of the geomagnetic total intensity were made at 46 points inside the volcano island and 45 points on the main land as shown in Fig. 4-1 respectively. Observations were also made along four tracks (T1, T2, T3 and T4) on Taal lake by boat.

The sensor of the proton magnetometer was at 2 m 28 cm height from the ground surface in the case of the observation on land. At each observation point, ten measurements of the total intensity were made.

For the observation on the lake, the sensor of the proton magnetometer was set about 2.5 m out the front of the boat. The observed values were

corrected because the observed values were affected by the magnetization of the boat, and the affected value amounted to about 20 nT. The observation were done while boating and the observed values were obtained as the average of about five measurments.

All observation values were reduced to the value at 00 h 00 m on January 25, 1980 (local time) at Muntinlupa Magnetic observatory. Namely, the reduced value F is expressed as follows;

$$F = F_O(t) - [F_M(t) - F_M(t_O)]$$

where $F_O(t)$ = total intensity at the time t for each observation point

$F_M(t)$ = one at t for Muntinlupa

$F_M(t_O)$ = one at oo h oo m on January 25, 1980 for Muntinlupa.

The observed values and reduced values on land are tabulated in Table 4-4 and the reduced values on the lake are shown in Fig. 4-4 and 4-5.

Table 4-4(1) Geomagnetic total intensity on and around Taal volcano.

Observation Point	Latitude (N)	Longitude (E)	Observed Value	Reduced Value	Date and Time (LT)
	° '	° '	nT	nT	1980 h m
V9A	13 59.78	120 58.58	40750	40705	Jan. 17, 9 9
TV1	13 59.81	120 58.92	40802	40747	17, 10 4
TV2	13 59.95	120 58.92	40614	40556	17, 10 20
TV3	14 0.00	120 59.08	41195	41139	17, 11 19
TV4	14 0.03	120 58.83	40214	40171	17, 12 9
DK1	14 1.90	120 59.94	40200	40181	18, 14 31
DK2	14 1.55	120 59.86	39727	39710	18, 14 50
TV5	14 1.28	120 59.89	40500	40484	18, 15 8
TV6	14 1.17	120 59.92	40975	40962	18, 15 45
DK3	14 1.22	120 59.93	39736	39724	18, 16 23
V2A	14 1.93	120 59.14	40254	(40214)	20, 8 20
V2B	14 2.04	120 58.72	40803	(40763)	20, 8 44
V1B	14 1.93	120 58.31	40781	(40741)	20, 9 13
V1A	14 1.41	120 58.33	40442	(40392)	20, 9 25
V10C	14 1.11	120 58.28	40648	(40598)	20, 9 35
V14B	14 0.30	120 58.33	40282	(40232)	20, 9 46
V9A	13 59.78	120 58.58	40765	(40715)	20, 9 59
V9B	13 59.18	120 58.94	40714	(40664)	20, 10 15
V8A	13 59.29	120 59.47	40734	(40684)	20, 10 34
V7A	13 59.54	121 0.08	40742	(40692)	20, 11 2
V6	14 0.03	121 0.72	40333	(40283)	20, 11 17
V6A	14 0.33	121 0.81	40741	(40691)	20, 11 30
V5B	14 0.68	121 0.94	40721	(40671)	20, 11 42
V5A	14 1.55	121 0.78	40742	(40692)	20, 11 59
V4	14 2.26	121 0.89	40746	(40706)	20, 12 13
V11B	14 2.60	121 0.97	40964	(40924)	20, 12 28
V11	14 2.34	121 0.58	39609	(39569)	20, 12 38
V3	14 2.26	120 59.68	40300	(40290)	20, 17 39
V3A	14 2.17	121 0.00	40941	(40931)	20, 17 55
ML1	14 5.41	121 1.44	40599	40574	21, 7 55
ML2	14 5.00	121 4.03	40447	40416	21, 8 12
ML3	14 6.06	121 5.83	40342	40295	21, 8 29
ML4	14 5.11	121 7.92	40590	40525	21, 9 13
ML5	14 4.40	121 6.19	40576	40511	21, 9 27
ML6	14 3.13	121 4.86	40370	40313	21, 9 43
ML7	14 3.61	121 8.81	40584	40524	21, 10 35
ML8	14 2.85	121 6.31	40280	40227	21, 10 49
ML9	14 2.12	121 9.72	40460	40408	21, 11 8
ML10	13 59.32	121 10.42	40238	40187	21, 11 25
ML11	14 6.30	120 58.14	40479	40457	21, 14 48
ML12	14 7.12	120 57.75	40301	40282	21, 15 15
ML13	14 7.55	120 59.39	40227	40207	21, 15 30
ML14	14 8.80	120 57.33	40354	40338	21, 15 47
ML15	14 11.27	120 57.70	40291	40275	21, 15 57
ML16	14 6.25	120 56.72	40303	40287	21, 16 21
ML17	14 6.28	120 54.54	40236	40223	21, 16 57

Table 4-4(2) Geomagnetic total intensity on and around Taal volcano.

Observation Point	Latitude (N)	Longitude (E)	Observed Value	Reduced Value	Date and Time (LT)
	° '	° '	nT	nT	1980 h m
ML18	14 5.16	120 52.86	40191	40180	Jan. 21, 17 8
ML19	14 4.02	120 50.86	40436	40426	21, 17 20
ML20	13 58.70	121 8.61	40370	40324	22, 8 39
ML21	14 0.76	121 7.56	40499	40448	22, 8 52
ML22	14 1.14	121 5.75	40307	40243	22, 9 20
ML23	13 57.83	121 10.00	40417	40348	22, 9 59
ML24	13 56.85	121 7.06	40471	40397	22, 10 18
ML25	13 58.13	121 6.17	40529	40453	22, 10 33
ML26	13 54.89	121 6.03	40512	40435	22, 10 55
ML27	13 53.34	121 5.81	40437	40358	22, 11 9
ML28	13 51.39	121 3.14	40397	40326	22, 11 52
ML29	13 52.26	121 1.11	40293	40225	22, 12 59
ML30	13 49.68	121 1.11	40227	40162	22, 13 13
ML31	13 51.66	120 59.17	40268	40213	22, 14 1
ML32	13 52.88	120 57.64	40504	40446	22, 14 22
ML33	13 54.32	120 56.03	40316	40262	22, 14 46
ML34	13 55.71	120 57.25	40226	40191	22, 15 27
ML35	13 53.99	121 3.25	40677	(40647)	22, 18 20
ML36	14 5.22	120 57.86	41097	41068	23, 8 17
ML37	14 4.35	120 56.97	40709	40676	23, 8 43
ML38	14 3.34	120 56.22	40442	40403	23, 9 24
ML39	14 4.86	120 57.56	40633	40584	23, 10 2
ML40	14 5.38	120 58.81	40448	40396	23, 10 24
ML41	14 5.16	120 59.64	40624	40571	23, 10 40
ML42	14 2.04	120 56.72	40376	40340	24, 8 19
ML43	14 0.87	120 57.08	40327	40285	24, 8 44
ML44	13 59.38	120 56.97	40103	40056	24, 9 7
ML45	13 58.37	120 56.69	40225	40170	24, 9 52
TV7	14 1.25	120 58.81	40468	40406	24, 11 10
TV8	14 1.41	120 58.61	40600	40539	24, 11 22
TV9	14 1.60	120 58.39	40590	40529	24, 11 32
V12	14 0.68	120 58.67	40589	40831	27, 9 18
V13A	14 0.63	120 58.99	40667	40637	27, 9 26
V15	14 0.54	120 59.36	40989	40963	27, 10 9
TV10	14 0.30	120 59.81	41224	41197	27, 10 24
TV11	14 0.73	120 59.44	40914	40903	27, 10 53
TV12	14 0.60	120 59.14	40606	40604	27, 11 21
TV13	14 0.72	120 58.85	40352	40360	27, 11 42
TV14	14 0,73	120 58.39	40502	40512	27, 12 5
TV15	14 1,71	120 59.21	40096	40087	28, 9 37
TV16	14 1.71	120 58.92	40377	40362	28, 10 2
TV17	14 1.44	120 58.82	40454	40443	28, 10 20
TV18	14 1.37	120 59.14	40403	40392	28, 10 43
TV19	14 1.60	120 59.21	40350	40343	28, 10 56
TV20	14 1.83	120 59.19	40296	40293	28, 11,12

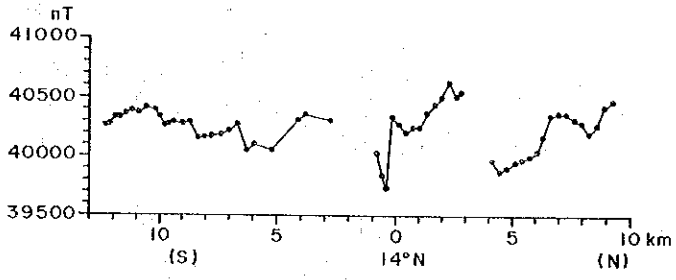

Fig. 4-4 Geomagnetic total intensity along the tracks of the boat on the Taal lake.

Observed values show large differences from point to point in some places, particulary on and near the volcano island. Then, small-scale anomalies are stripped and largescale anomalies are outlined in Fig. 4-6.

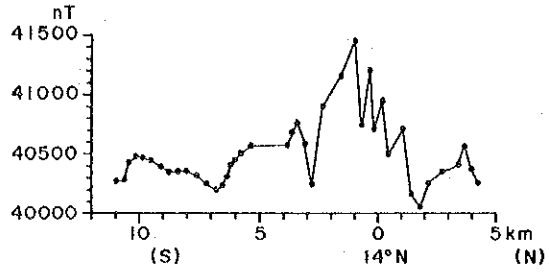

Fig. 4-5 Geomagnetic total intensity along the track of the boat on the Taal lake.

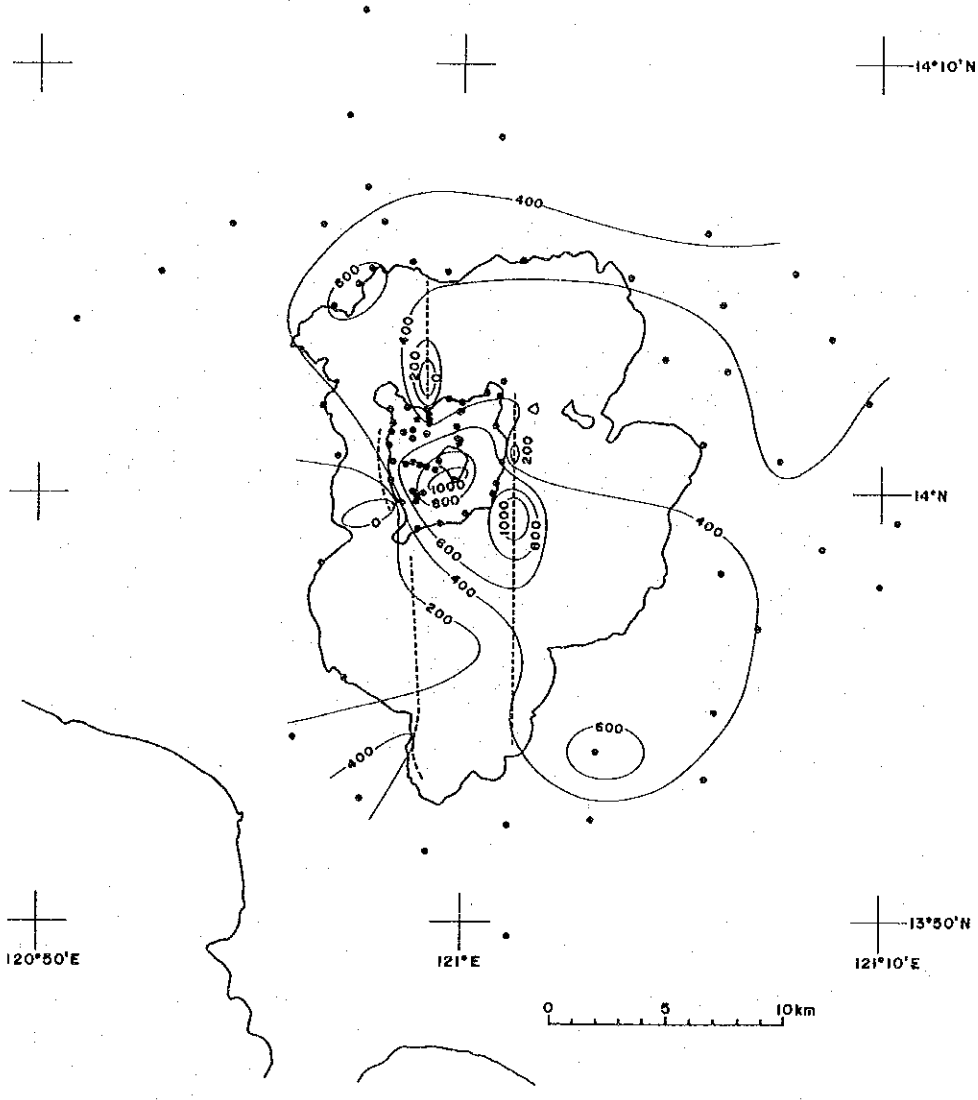

Fig. 4-6 Distribution of the geomagnetic total intensity on and around Taal volcano. Values are given in nT. Real values are obtained by adding 40,000 nT to the values in the figure.

In Fig. 4-6, the following anomalies can be seen.

(a) A negative anomaly of about 400 nT in the lake near the north-western volcano island.

(b) A positive anomaly of about 600 nT over the Main Crater Lake and New Eruption Site.

(c) A positive anomaly of about 600 nT in the lake near the south-eastern volcano island.

(d) A negative anomaly of about 200 nT in the lake near the south-western volcano island.

(e) A negative anomaly of about 200 nT in the lake near the eastern volcano island.

4. Interpretation about magnetic anomalies on and around Taal volcano

The intensity of the magnetic field f at a point (x, y, z) due to a magnetic dipole M whose direction-cosines are λ, μ and ν is given by

$$f = [\{\alpha F + \frac{M}{r^3}(-\lambda + \frac{3kx}{r^2})\}^2 + \{\beta F + \frac{M}{r^3}(-\mu + \frac{3ky}{r^2})\}^2 + \{\gamma F + \frac{M}{r^3}(-\nu + \frac{3kz}{r^2})\}^2]^{1/2}$$

where F is the total intensity of the earth's normal field which is characterized by the direction-cosines α, β and γ.

And $k = \lambda x + \mu y + \nu z$

$r^2 = x^2 + y^2 + z^2$

So, the total force anomaly ΔF is as follows;

$\Delta F = f - F$

Fig. 4-7 shows the distributions of the total force anomaly due to a dipole at a depth of 2, 3, 4 and 5 km, where the direction of the magnetic moment amount of 2×10^{14} emu, lies in the magnetic meridian plane and that it's inclination agrees with the geomagnetic dip which is taken as 14°. The total intensity of surrounding area is assumed as 40,400 nT. As Fig. 4-7 shows, a negative anomaly is rather correspond to a magnetized body in the low latitude.

The negative anomaly in the north-west direction of the volcano island is similar to the anomaly at the depth of 3 km in Fig. 4-7. If the specific

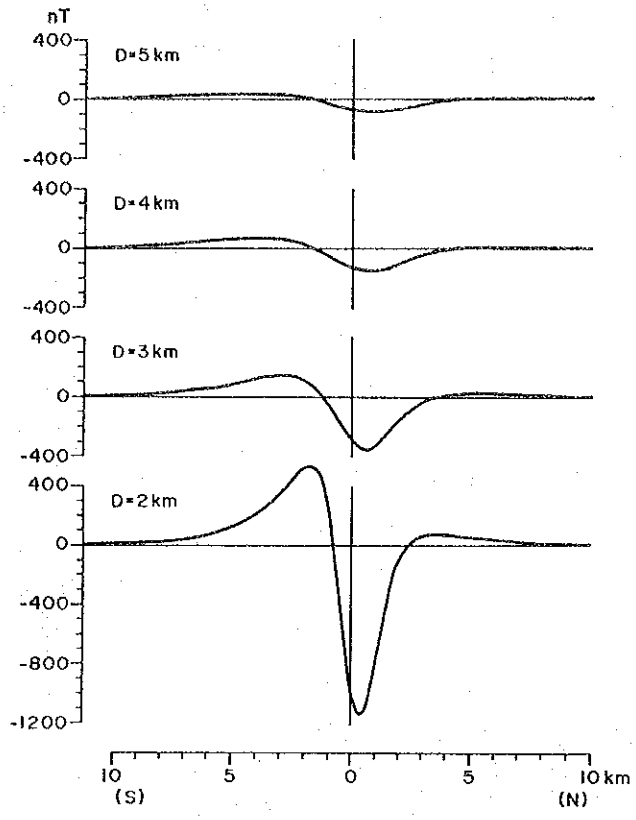

Fig. 4-7 Distributions of the magnetic total force anomalies due to a magnetic dipole. It's intensity and inclination is 1×10^{14} emu and 14° respectively.

intensity of the magnetization is taken as 5×10^{-2} emu/cc, the causative body is correspond to a magnetized sphere having a diameter 1,560 m.

The positive anomaly over the Main Crater Lake and New Eruption Site is considered to show that the temperature of underground lava is still high above the Curie Point. This view is consistent with the fact that high gravitic area [16] and high tempereture area exist in this poiitive anomalous area.

The anomaly in the lake near the south-eastern island is similar to the preceding one. It indicates a possibility of demagnetization due to heating, but there is no other additional information.

One of the causative body of the negative anomaly in the south-west direction of the island is considered to be the 1969 lava flow cooled by the water of the lake.

Also, it seems that lava are irregularly distributed under the lake to the east of the island from the fact that the observed values are very scattering as seen in Fig. 4-5.

The volcano island is composed almost of the pyroclastic materials which are the product of past magmatophreatic eruptions and we can not see lava flow except a small part of the north-eastern coast and the south-western part of the volcano island. Near the point TV10 which is located on the shore of the Main Crater Lake and just under the cliff with about 10 m high, the observed total intensities were almost the same value even if we moved the sensor of the proton magnetometer within few meters in distance. From this fact, the magnetization of the pyroclastic materials around here are seemed to be very weak.

If we assume that the pyroclastic materials which cover the volcano island are hardly magnetized, it can be considered that the cause of the small-scale anomalies of the total intensity are origined from masked volcanic rocks.

Accordingly, it is expected that more high-dense magnetic observation may find out the distribution of high magnetized volcanic rocks.

5. Magnetic gradient

Generally in a volcanic area, intensity of geomagnetic field is varied from place to place, because of irregular distribution of high magnetized rocks and/or effect of complication of the topography. On the contrary, we can not expect that remarkable changes of geomagnetic field caused by thermal and pressure effects within a short period of time except the case of quick crustal movements.

A few instances are given to show how different the total intensity is in different point.

Near the point V3A close to the old lava flow in Taal volcano, the differential field in the total intensity amounted 1,500 nT between two points at a distance only 20 m apart.

In Bulusan volcano, total intensities were observed on flat ground and around a exposed rock. In the case of the formar, the differential fields

in the total intensity were within only 3.3 nT in the space of 2 m × 1 m wide and 1.74 - 2.34 m high.

In the latter case, when we measured the total intensities at the level of 2 m on the north and south sides of the exposed rock which have about 2 m in apparent diameter and about 50 cm in height, the differential field amounted to about 50 nT. This indicates that magnetic field is strongly disturved by the magnetization of the exposed rock.

There are some magnetized rocks just under the surface even on outwardly flat ground, so it is necessary to avoid on the place such that magnetic field steeply changes. It is more important to set up the sensor of magnetometer exactly to the same position in the case of repetition of magnetic survey.

Observed values in the total intensity do not change strongly within the area of 5 m × 2 m wide around the magnetic point near the Mayon Rest House Observatory. But this point is undesirable for the magnetic point to detect volcanomagnetic effect because the point is close to magnetized artifitial constructions.

6. Repeated magnetic survey around Bulusan volcano

In order to detect a geomagnetic changes associated with the volcanic activity, magnetic survey was repeated around Bulusan volcano.

Three magnetic observation points were located at Cogon on the southwestern foot of Bulusan volcano and two points at San Benon on the southern foot of the volcano. The points at Cogon spaced with about 500 m interval and the points at San Benon with about 200 m interval.

Differential field between two points were measured several times in short period because only one magnetometer was used. The results are tabulated in Table 5. Each value is the average of ten measurments. Unfortunately the survey was not able to do only two times because of the trubles of the magnetometer.

As the result, clear geomagnetic change associated with the volcanic activity was not detected.

Table 4-5 Result of repeated magnetic survey around Bulusan volcano

Location	Date	Point No.	Time (LT)	Observed Value	Local Difference	Mean
			h m	nT		
		B1	9 16	39417.1	nT	nT
		B2	30	39433.5	B2-B1= 11.1	B2-B1= 10.2
	1980	B1	38	39423.9	B2-B1= 9.3	
	Feb. 8	B2	45	39432.9		B3-B2=258.2
		B3	54	39691.3	B3-B2=258.9	
		B2	10 8	39431.5	B3-B2=257.5	B3=B1=268.4
		B3	15	39687.9		
Cogon		B1	25	39427.7		
			h m	nT		
		B1	9 16	39441.0	nT	nT
		B2	24	39450.1	B2-B1= 6.9	B2-B1= 7.1
	Feb. 11	B1	30	39445.1	B2-B1= 7.3	
		B2	36	39454.7		B3-B2=261.6
		B3	44	39719.5	B3-B2=262.3	
		B2	52	39459.7	B3-B2=260.8	B3-B1=268.7
		B3	59	39720.5		
		B1	10 9	39452.6		
			h m	nT		
		B4	16 3	39638.4	nT	
		B5	11	39598.4	B5-B4=-40.1	nT
	Feb. 8	B4	15	39638.5	B5-B4=-41.3	B5-B4=-41.3
		B5	21	39595.3	B5-B4=-42.5	
San Benon		B4	26	39637.3		
			h m	nT		
	Feb. 11	B4	11 40	39732.7	nT	
		B5	52	39688.9	B5-B4=-41.9	
		B4	55	39730.3		

§5 Conclusion

By the Joint Research Work with the COMVOL, we conducted field inspections at mainly volcano Taal, with a seismograph, an IR thermometer and a magnetometer. The brief of results of inspections is as follows;

(1) At volcano Taal, seismic activity was in low frequency, but volcanic earthquakes called "type S" which are considered to occure at rather deep site at active volcanoes were taken place at the rate of 0.4/ day & 11-12/ month in recent years of 1979 & 1980, according to the seismological observations at Pirapiraso observatory.

(2) Unequal distribution of ground vibration inside Taal volcano island was confirmed by field inspections with the portable seismograph. It was also confirmed that amplitude-distribution of the continuous waves was larger in the western side of this volcano than the amplitudes in the eastern side.

(3) The amplitude-distribution of ground-vibration inside volcano Taal obtained by field inspections by the COMVOL in 1978 showed the almost same tendency as our results. It was seen that the amplitude has been decreasing in recent years, according to analysis of the periodical inspections conducted by the COMVOL since 1977 through 1979.

(4) It, however, is hard to conclude that those continuous waves obtained by this research work are typical volcanic tremors which occure at Taal volcano. The further investigations by using analysis of horizontal components of waves are necessary on this matter.

(5) Volcanic events were not obtained at volcanoes of Mayon and Bulusan with the portable seismograph. Ordinary ground vibrations at both of volcanoes were in rather high amplitude owing to surrounding conditions.

(6) By the seismological observation of the COMVOL at volcano Bulusan, precursory increase of volcanic tremors & volcanic earthquakes of "type S" were confirmed prior to the occurrence of volcanic explosions on February 7-9, 1980.

(7) Explosion-tremor generated by the explosion on February 7, 1980 of volcano Bulusan was analyzed with the seismogram by the Ranger type seismograph. The energy-release was estimated to be magnitude less than 0.7 and

energy of 10^{11-12} erg..

(8) High temperature areas/geothermal anomalies are located at the New Eruption Site, around B. Malaqui, at the shore-side of Mt. Balantoc and around the inner wall of Main Crater at volcano Taal. There was no geothermal anomaly in the eastern side of this volcano.

(9) Geothermal anomalies at Main Crater and the New Eruption Site are distributed in a direction of NE-SW. Direction of the distribution of 1976 & 1977 craters is also NE-SW. The direction at the central part of this volcano may represent the underground tectonic structure of volcano Taal.

(10) Estimation of heat-flux based on measurements of surface temperatures at volcano Taal was tried and the result was 3.24×10^6 cal/ sec. The amount of the heat-flux belongs to active thermal activities comparing examples of active volcanoes in Japan.

(11) By analysis of the infrared images of volcano Taal obtained in 1965 by airborne infrared scanner, it was seen that locations of the geothermal anomaly in volcano island in 1965 was almost same as the result in (8). But the width of high temperature areas of our result is smaller than those in 1965, and it is considered that geothermal activity decreased in recent years.

(12) There was not remarkable change of water-temperature of hot-springs located at the foot of volcano Bulusan during this eruptive activity.

(13) From both of results of seismological & geothermal inspections, it is considered that active areas of volcano Taal are distributed in the western side in this volcano island. Not only the New Eruption Site, but also areas of B. Malaqui and Mt. Balantoc should be noticed owing to high geothermal anomaly as future active sites.

(14) It is concluded that volcano Taal is now in calm state, but occurrence of "type S" volcanic earthquakes and existence of active geothermal anomaly show underground active state of this volcano.

(15) Magnetization of the lava flow in volcano Taal is very strong. The intensity of the NRM of the 1969 lava flow is about 5×10^{-2} emu/cc and one of the lava flow of the north-eastern coast about 1×10^{-2} emu/cc.

(16) Observations of the geomagnetic total intensity were made on Taal volcano island, Taal lake and the main land, and five remarkable anomalous regions are found.

(17) The positive magnetic anomaly over the Main Crater Lake and New Eruption Site is considered to show that the temperature of underground lava is still high.

(18) The positive anomaly in the lake near the south-eastern side of Taal volcano island may suggest the existence of high temperature material under the ground. It is desirable to make more detailed investigation.

(19) In the case of the magnetic survey by COMVOL, the corrections of the magnetic disturbances such as diurnal variation, magnetic storm and like have been done by using observed value at a base station within the survey area. The volcanomagnetic effect could be detected by the method that a sensor of a magnetometer occupies exactly the same space for each survey.

(20) Furthermore, if the result of the magnetic survery was compared with the value at a standard magnetic observatory, magnetic conditon in the wide area involving Taal volcano island and/or Taal lake could be searched.

(21) Magnetic survey was repeated around volcano Bulusan, but clear geomagneitc change associated with the volcanic activity was not detected.

Acknowledgement

First, we would like to express for ourselves our sincerest thanks and appreciation for the amount of efforts put forth by the staff members of the Philippine Commission on Volcanology, National Science Development Board. They provided for field works & discussions during the research inspections, and oppotunities to visit the COMVOL facilities at Taal, Mayon and Bulusan volcanoes and to investigate the seismological events by sending of materials of routine observational works by the COMVOL. We are grateful to Mr. C. M. Santos and the staff members of the Bureau of Coast and Geodetic Survey for providing copies of the magnetograms of Muntinlupa Magnetic Observatory.

At the same time, we express our cordial thanks to the officials of Ministry of Foreign Affairs of Japan, Ministry of Transport of Japan, Japan Meteorological Agency and Japan International Cooperation Agency for their efforts concerning this Joint Research Work on volcanic activities in the Philippines.

We would like to thank Mr. I. Fujisawa and the officials of Volcanological Office, Seismological Division, Japan Meteorological Agency for the permission of usage of instruments of the seismograph. We would like to thank Prof. I. Aoyama, Tokai University for offering convenience to use the proton precession magnetometer and Dr. T. Nakatani, University of Tokyo for the magnetic examination of rock samples.

During the Joint Research Work, Mr. O. Peña, the Deputy Commissioner and Mr. E. Villalva, the Chief Scientist, the COMVOL always provided us their warmful and technical efforts. Many staff members of the COMVOL attended this Reseach Work to operate the field inspections as follows; Mr. A. Oanes, Mr. C. Vicente, Mr. E. Dela Cruz, Mr. D. Marzan, Mr. D. Garcia, Mr. A. Almeda, Mr. R. Lizardo, Mr. R. Crisostomo and Mr. O. Rosales from the Main Office, Mr. C. Andal, Mr. R. Mayuga, Mr. J. Ventura and Mr. S. Cesario from Pirapiraso Observatory, Taal and Mr. J. Barera from St. Mesericordia Observatory, Mayon. We cordially thank their cooperation.

Reference

(1) K. Nakamura (1966): The Magmatic Eruption of Taal Volcano in 1965, Philippines, Journal of Geography, Vol.76, 93-104 (in Japanese with English abstract)

(2) J. G. Moore, K. Nakamura and A. Alcaraz (1966): The 1965 Eruption of Taal Volcano, Science, Vol.151, No.3713, 955-960

(3) Y. Sawada and T. Mori (1980): Brief Report on Volcanological Research Work in the Philippines, 1-18 (in Japanese), unpublished

(4) Y. Sawada and T. Mori (1980): Brief Report of the Joint Research Work on Volcanic Activity in the Philippines, 1-22, unpublished

(5) Commission on Volcanology (1968): Taal since its Eruption of August, 1967-Seismicity, The COMVOL Letter, Vol. I, No.5, 3-4

(6) I. Yokoyama (1956): Energetics in Active Volcanoes, 1st Paper (Activities of Volcano Mihara, Ooshima Island during the Period 1953-1954), Bulletin of Earthq. Res. Inst., Vol.34, 185-195

(7) M. Sekioka and K. Yuhara (1974): Heat Flux Estimation in Geothermal Areas, Based on the Heat Balance of the Ground Surface, Journal of Geophysical Research, Vol.79, No.14, 2053-2058

(8) G. A. Briggs (1969): Plume Rise, Critical Review Series, Rep. TID-25075, At. Energy Comm., Washington, D. C.

(9) T. Kagiyama (1978): Evaluation of Heat Discharge and H_2O Emmission from Volcanoes —— Based on a Plume Rise Assumption ——, Bull. Volcanological Society of Japan, II, Vol.23, 183-197 (in Japanese with English abstract)

(10) R. M. Moxham and A. Alcaraz (1966): Infrared Surveys at Taal Volcano, Philippines, COMVOL Annual Report, Manila, 78-85

(11) R. M. Moxham (1966): Changes in Heat Flow at Taal Volcano, Philippines from October, 1965 to May, 1966, COMVOL Annual Report, Manila, 87-93

(12) L. G. Aguila (1978): The 1978 Eruptions of Bulusan Volcano, The COMVOL Letter, Vol. 10, Nos.3 & 4, 4-8

(13) A. F. Oanes and D. J. P. Marzan (1978): Magnetic and Gravity Survey of Taal Volcano, Technical Reports, COMVOL, 6-11

(14) N. C. Baligod (1978): Magnetic Survey of Mayon Volcano, Technical Reports, COMVOL, 21-22

(15) J. S. Sincioco (1979): Magnetic and Gravity Surveys of Taal Volcano Island, unpublished

(16) I. Yokoyama, A. Alcaraz and O. Peña (1975): Gravimetric Studies of Taal Volcano, Philippines, Bulletin Volcanologique, Tom. XXXIX-3, 1-11